sustainability

MDPI

Article

Sustainable Hydrogen from Palm Oil Rachis: A Techno-Environmental-Economic Assessment for Palm Rachis Gasification in Colombian Post-Conflict Rural Territories

Paola Andrea Acevedo Pabón [1], Tamy Carolina Herrera-Rodríguez [2] and Ángel Darío González-Delgado [2,*]

[1] Chemical Engineering Department, Faculty of Engineering, Universidad EAN, Carrera 11 #78-47, Bogotá 111321, Colombia; paacevedo@universidadean.edu.co
[2] Nanomaterials and Computer Aided Process Engineering Research Group (NIPAC), Chemical Engineering Department, Universidad de Cartagena, Avenida del Consulado Calle #30 No. 48 152, Cartagena 130015, Colombia; therrerar@unicartagena.edu.co
* Correspondence: agonzalezd1@unicartagena.edu.co

Abstract

The global push for energy decarbonization has increased interest in hydrogen as a clean energy carrier. Biohydrogen from agricultural residues is a promising pathway for countries with strong agro-industrial sectors. This study evaluates the technical, economic, and environmental feasibility of hydrogen production from palm oil rachis in two post-conflict regions of Colombia: a large-scale facility in Bolívar and a small-scale plant in Santander. The assessment integrates Aspen Plus® (version 14) simulations using the NRTL thermodynamic model, an attributional gate-to-gate Life Cycle Assessment (LCA) with ReCiPe Midpoint (H), and a techno-economic analysis. The simulated process includes biomass drying, decomposition, steam gasification, syngas cleaning, and methane reforming. A key technical finding was the non-linear relationship between feedstock composition and process yield. Although Santander's biomass had a higher hydrogen content (9.42% vs. 6.58%), Bolívar achieved a much higher conversion efficiency (0.198 kg H_2/kg biomass) and produced over seven times more hydrogen while processing only 5.8 times more biomass. Environmental results showed clear advantages for Bolívar, which presented lower impacts across most categories compared to Santander and the fossil-based hydrogen benchmark. Bolívar achieved a Global Warming Potential of 2.47 kg CO_2 eq/kg H_2, far below the 15.03 kg CO_2 eq/kg H_2 of Santander, and showed favorable performance in particulate matter formation, acidification, and fossil resource scarcity. Economically, Bolívar was viable, with a Net Present Value of USD 25.01 million, a Benefit–Cost Ratio of 3.29, and a discounted payback period of 4.54 years. Santander was economically unfeasible under all conditions. Hydrogen production from palm rachis is technically feasible, environmentally beneficial, and economically viable when biomass availability and process integration are adequate, as illustrated by the Bolívar case.

Keywords: biohydrogen; biomass gasification; oil palm rachis; life cycle assessment (LCA); techno-economic analysis; process simulation; Aspen Plus

Academic Editor: Lucília Graciosa de Sousa Ribeiro

Received: 7 December 2025
Revised: 16 January 2026
Accepted: 26 January 2026
Published: 6 February 2026

1. Introduction

The escalating global challenge of climate change, driven by extensive reliance on fossil fuels, has underscored the urgent need for sustainable, clean energy alternatives. In response, hydrogen (H_2) has emerged as a promising clean energy carrier due to its high

gravimetric energy density and the fact that its combustion by-product, water (H_2O), is free of carbon dioxide (CO_2) and other harmful pollutants [1]. Biomass, as a carbon-neutral resource with rapid biogeochemical cycles, offers a viable and sustainable pathway for H_2 production through thermochemical conversion processes, such as gasification. This approach not only mitigates net greenhouse gas emissions but also provides a strategic means of managing agricultural waste.

Colombia, with its significant agricultural sector, generates substantial biomass residues, particularly from the palm oil industry. This biomass, specifically the empty fruit bunches (rachis), represents a valuable and underutilized resource for energy generation and chemical production [2,3]. Converting these residual biomasses into high-value products, such as H_2, can create economic opportunities and support the development of rural territories, especially in post-conflict zones, where sustainable economic activities are crucial to stability and social progress [4]. The selection of Bolívar and Santander as case studies is deeply rooted in Colombia's socio-political context. These regions were historically among the territories most severely affected by the internal armed conflict, enduring decades of instability due to the presence of guerrilla groups (FARC-EP, ELN) and paramilitary forces (AUC), which significantly hindered agro-industrial development and led to land abandonment. In the current post-conflict era, the implementation of hydrogen production from agricultural residues represents more than an energy transition strategy; it acts as a mechanism for territorial reconstruction. By fostering a circular bioeconomy around palm oil rachis, this technology aims to generate high-skilled employment and new revenue streams, aligning with national policies to leverage science and technology to consolidate peace and promote sustainable industrialization in regions previously isolated by war. There are various conversion pathways for generating biohydrogen from oil palm rachis: conversion processes can be broadly categorized into thermochemical pathways—such as gasification, pyrolysis, and supercritical water gasification (SCWG)—and biochemical routes, including dark fermentation, anaerobic fermentation in sequencing batch reactors, and emerging hybrid systems that combine biological and electrochemical processes [5]. Gasification was selected as the primary conversion pathway due to its distinct technical advantages for processing complex lignocellulosic feedstocks such as palm rachis. Unlike biological routes, which often require extensive enzymatic pretreatment and have slower reaction rates, gasification offers rapid reaction kinetics and high conversion efficiencies. Furthermore, it enables high-grade heat recovery and thermal integration, and, when coupled with Water–Gas Shift (WGS) and reforming units, significantly increases hydrogen yields by fully valorizing the feedstock's carbon content. Oil palm rachis is a lignocellulosic biomass characterized by a substantial content of cellulose, hemicellulose, and lignin, with typical compositions reported as approximately 38% cellulose, 21% hemicellulose, and 16% lignin [6,7]. These structural carbohydrates render the feedstock amenable to various conversion processes, making it suitable for both direct thermochemical transformation and pretreatment followed by biochemical fermentation [7]. The proximate and ultimate analyses of oil palm rachis also indicate high volatile matter content and a relatively higher heating value, which are favorable properties for gasification reactions [6,7]. Given the enormous global production of oil palm biomass, its conversion into biohydrogen not only represents a significant renewable energy opportunity but also helps mitigate environmental impacts associated with waste disposal and open burning [5,8]. Oil palm rachis, technically known as Empty Fruit Bunches (EFBs), are the most significant lignocellulosic byproduct of the palm oil agro-industry, accounting for approximately 22% of the total mass of Fresh Fruit Bunches (FFBs) processed. Globally, the generation of this residue is estimated to exceed 87 million tonnes per year, representing a substantial yet underutilized biomass resource. While currently used primarily for low-value soil mulching or

left to decompose—often generating methane emissions—its physicochemical properties make it an ideal candidate for energy valorization. With a Lower Heating Value (LHV) of 18.8 MJ/kg (dry basis), rachis has an energy density comparable to that of lignite coal. Consequently, the thermochemical conversion of this residue not only provides a renewable energy source (1 ton of EFB is energetically equivalent to approximately 5 GJ) but also significantly mitigates the carbon footprint, potentially avoiding 0.9–1.0 kg of CO_2eq per kilogram of rachis, thereby replacing fossil feedstocks.

Thermochemical conversion pathways are robust methods that decompose biomass by applying high temperatures in controlled environments, releasing gaseous products that can be further refined into biohydrogen. Gasification is the most widely studied thermochemical process for biohydrogen production from oil palm rachis, in which the biomass is converted to synthesis gas (syngas) via partial combustion at elevated temperatures [7]. Biohydrogen produced via biomass gasification is increasingly recognized as a promising renewable energy carrier due to its potential to deliver low- or even negative-carbon outcomes when appropriately designed. In a typical gasification process, oil palm rachis is dried, milled, and fed into a gasifier where it undergoes sequential reactions starting with pyrolysis (thermal decomposition in the absence of oxygen) and followed by oxidation and reduction reactions that yield a mixture of hydrogen, carbon monoxide, carbon dioxide, and minor species such as methane [5]. The produced syngas contains an appreciable hydrogen concentration, which can be purified via catalytic reforming and Water–Gas Shift reactions, in which carbon monoxide reacts with steam to produce additional hydrogen and carbon dioxide. The operational parameters in gasification, such as temperature (typically within 800–900 °C), equivalence ratio, and the gasifying agent (air, oxygen, or steam), have been optimized in various studies to maximize hydrogen yield while controlling tar formation and char production [5,7]. Moreover, the choice of reactor configuration (fixed-bed, fluidized-bed, or downdraft gasifier) significantly influences heating rates and mixing characteristics, which, in turn, affect the overall syngas composition and the efficiency of downstream catalytic steps for biohydrogen extraction [5,7].

To holistically evaluate the feasibility of such processes, a comprehensive assessment framework that goes beyond technical and economic viability is necessary. The Life Cycle Assessment (LCA) methodology is a powerful tool for evaluating the potential environmental and social impacts of a product or process throughout its entire life cycle. Environmental LCA (E-LCA) quantifies environmental burdens, including climate change, acidification, and resource depletion [9,10]. This paper presents a comprehensive sustainability evaluation of H_2 production from palm oil rachis in Colombian contexts, focusing on two palm oil extraction plants in distinct post-conflict regions. The study combines process simulation with a detailed life cycle assessment to provide a robust analysis. It aims to characterize the biomass feedstock from these two locations and use this data to model the thermochemical gasification process for H_2 production. Subsequently, an E-LCA will be conducted using SimaPro 10.2, integrating the ReCiPe Midpoint (H) method and Ecoinvent 3 database data for environmental inventory analysis. The goal is not only to assess the technical feasibility and environmental benefits of this process but also to elucidate its environmental and economic contributions to regional development. Beyond comparison, this study examines the conditions under which the process is feasible, and the environmental indicators are lower than those for conventional hydrogen production processes. This integrated approach serves as a benchmark for similar evaluations in other agricultural contexts and provides a solid foundation for promoting sustainable territorial growth in Colombia's post-conflict areas.

2. Materials and Methods

2.1. Process Modeling and Simulation

The primary objective of the simulation is to establish a robust technical and operational foundation for the proper sizing of the equipment involved in hydrogen production from two distinct biomass sources. The model aims to accurately represent the sequential stages of drying, decomposition, gasification, gas cleaning, and steam methane reforming for hydrogen generation, which are essential for defining the capacity, operating conditions, and technical specifications of each process unit. Beyond validating the technical feasibility of the proposed process configuration, the simulation also enables optimization of operating conditions to maximize hydrogen yield while minimizing by-product and residual-stream generation [11].

Thermodynamic model selection: In simulating hydrogen production from rachis biomass, selecting an appropriate thermodynamic model is essential to accurately represent the complex liquid-phase interactions arising from biomass-derived streams. The Non-Random Two-Liquid (NRTL) model is particularly well suited for this purpose due to its proven accuracy in highly non-ideal systems, such as those encountered in thermochemical conversion of rachis in hydrothermal liquefaction, pretreatment, or bio-oil separation processes [12]. These mixtures, primarily composed of water, organic acids (acetic and formic), alcohols (ethanol and methanol), ketones, furfural, and phenolic compounds, exhibit substantial deviations from ideality due to pronounced intermolecular interactions [13].

The NRTL model captures these complexities through the calculation of excess Gibbs free energy using binary interaction parameters (τ_{ij}) and a non-randomness factor (α), which typically ranges between 0.2 and 0.3 for biomass-derived systems, reflecting their partially ordered molecular structure [14]. For instance, during the simulation of bio-oil separation in a distillation column operating at 1 atm and 98 °C, NRTL accurately predicts the formation of two liquid phases at equilibrium: an aqueous phase (~92% water, 8% acetic acid) and an organic phase enriched in furfural and alcohols. This predictive capability is critical, as models based on Raoult's law or the Wilson equation may yield errors exceeding 30%, potentially compromising the design of separation units and adversely affecting mass balances for downstream operations such as aqueous-phase reforming [15].

Multiple studies indicate that NRTL reduces equilibrium-composition errors to approximately ±2–3% relative to experimental data, thereby substantially improving simulation reliability [16–18]. This accuracy enables the optimization of operating conditions, such as temperature, pressure, and water-to-biomass ratio. It enhances overall process efficiency, achieving up to 12% increases in hydrogen production relative to less representative thermodynamic models [19]. For these reasons, the NRTL model constitutes the technically optimal choice for representing phase equilibria in the conversion of rachis to hydrogen.

Biomass characterization: Physicochemical characterization was conducted on composite samples collected from biomass processing centers in Santander and Bolívar during the November 2024 harvest season. The samples were conditioned and analyzed by the certified Energy Science Laboratory at the Universidad Nacional de Colombia. The analyses were conducted under controlled conditions and in accordance with standardized methodologies (UNE, ASTM, and SM-2540-G). Although the results are reported on a dry basis (DB), the original material contains approximately 45% moisture; therefore, values can be adjusted to a wet basis (WB) by applying the corresponding correction factor. The process simulation assumes a total biomass feed rate of 3919 kg/h, which is the rachis generation flow in a real plant in Santander.

The composition data for Santander (Table 1) were incorporated into the simulation via the NS-SOLID stream, using the ULTANAL attribute to specify the elemental composition. The particle size distribution (PSD) was specified between 20 and 200 nm, with 10 nm

increments. A crusher operating at 20 kW was modeled to achieve the desired particle size reduction. Subsequently, the biomass was heated to 75 °C to simulate the drying process. This stage was supplied with an air stream of 1020 kg/h at 100 °C. Sensitivity analysis indicated that these operating conditions reduce the biomass's moisture content to below 1% [3]. Biomass conditioning involves drying and size reduction, so in the simulation, the comminution stage is modeled as a closed-loop grinding circuit. While a single-pass grinder often yields a broad particle-size distribution that requires downstream sieving, this study assumes an industrial configuration in which oversized particles are mechanically recirculated to the mill and fines are retained. Consequently, biomass losses during physical pretreatment are considered negligible for mass-balance purposes, with the aim of achieving a target particle size suitable for gasifier hydrodynamics, while the energy penalty associated with this recirculation is accounted for in the pretreatment section's overall electricity consumption.

Table 1. Dry-basis composition of rachis from Santander.

Parameter	Method/Standard	Units	Results	Uncertainty
Carbon (C)	UNE-EN 15407	% (DB)	47.72	±4.77
Hydrogen (H)	UNE-EN 15407	% (DB)	9.42	±0.94
Oxygen (O)	ASTM D5622-95	% (DB)	35.75	±3.57
Nitrogen (N)	UNE-EN 15407	% (DB)	1.42	±0.14
Sulfur (S)	Thermo Scientific (App Note 42151)	% (DB)	<0.10	±0.01
Fixed Solids	SM-2540-G	% (DB)	5.69	±0.68

On the other hand, the elemental composition of the second rachis sample obtained from a palm oil extraction plant at Bolivar (Colombia) (Table 2) was determined by the same laboratory. In this case study, the biomass feed rate was 22,844 kg/h, representing the rachis production in a real plant located in Bolivar. The characterization followed standardized analytical methodologies, including UNE-EN 15407 for carbon, hydrogen, and nitrogen [20]; ASTM D5622-95 for oxygen [21]; SM-2540-G for fixed solids; and Thermo Scientific Application Note 42151 for sulfur quantification [22]. Results are reported on a dry basis.

Table 2. Dry-basis composition of rachis from Bolivar.

Parameter	Method/Standard	Units	Results	Uncertainty
Carbon (C)	UNE-EN 15407	% (DB)	49.77	±4.98
Hydrogen (H)	UNE-EN 15407	% (DB)	6.58	±0.66
Oxygen (O)	ASTM D5622-95	% (DB)	40.80	±4.08
Nitrogen (N)	UNE-EN 15407	% (DB)	1.47	±0.15
Sulfur (S)	Thermo Scientific (App Note 42151)	% (DB)	<0.10	±0.01
Fixed Solids	SM-2540-G	% (DB)	1.39	±0.68

Nevertheless, the composition of both rachis samples reveals notable differences that influence their behavior in thermochemical conversion processes. The uncertainty values reported in Tables 1 and 2 correspond to the analytical uncertainty of the instrumentation and standardized methods used (including UNE-EN-15407 for elemental analysis and ASTM D5865M for calorific value), ensuring the reliability of the input data for the thermodynamic simulation. Although biomass composition naturally fluctuates due to seasonal and agro-climatic variables, these characterizations were established as the fixed design

basis to ensure mass-balance consistency throughout the process simulation. The Bolivar sample exhibits higher carbon (49.77%) and oxygen (40.80%) content than the Santander sample, suggesting greater potential for syngas generation and higher overall reactivity during gasification. Conversely, the Santander sample presents a significantly higher hydrogen content (9.42% vs. 6.58%), which may enhance the H_2/CO ratio in reforming processes but also indicates a more volatile-rich structure. Moreover, the ash content is considerably lower in the Bolivar sample (1.39% versus 5.69% in the Santander sample), implying a reduced risk of slagging, fouling, and catalyst deactivation during hydrogen production. Despite these variations, both samples exhibit similar nitrogen and sulfur levels, suggesting comparable tendencies for NOx and SOx formation. Overall, the Bolivar biomass appears more favorable for thermochemical hydrogen production due to its higher carbon content and lower ash fraction. In contrast, the Santander sample may perform better in processes where volatile components play a critical role.

Process Description

The modeled processes have the same number of equipment units; the difference lies in the processing capacity of the Bolívar case relative to that of the Santander case. Likewise, Santander requires a dryer and a mill with much smaller specifications because the biomass enters at a size that is easier to handle. In the diagrams, the equipment shown in yellow indicates the differences in equipment specifications.

The process begins by drying the rachis to remove moisture. Then, the biomass is milled to facilitate its transformation in subsequent stages. The milled rachis (stream 4) is sent to a gasification stage, where steam (stream 12) is supplied, producing a mixture of compounds (C, H_2, S, CO, CO_2, H_2O, CH_4, among others). The resulting stream (stream 13) from gasification is sent to a separator, where a mixture of water with carbon traces is removed. Subsequently, the process stream (stream 15) is fed to a compressor, where the pressure is increased as required for the high-temperature and low-temperature reactors, the absorption tower, and the PSA unit. Stream 17, composed mainly of methane, sulfur oxide, and carbon monoxide, is sent to a gas-washing stage in which condensable gases are retained, while the non-condensable gases (stream 24) are sent to continue the hydrogen reaction and purification process. The stream resulting from gasification (stream 27) is sent to a heat-exchanger train to raise the temperature of stream 6 before entering separator 2. In this equipment, stream 7, composed of water with traces of CO_2 and SO_2, is obtained. Stream 8 is then fed to the PSA unit, where hydrogen (stream 9) is purified and separated from the other synthesized gases (stream 10).

In the Bolívar process, from 22,884 kg/h of rachis, 4542.41 kg/h of hydrogen is produced; in the Santander process, from 3919.04 kg/h, 634.71 kg/h of hydrogen is produced. Figures 1 and 2 present the equipment diagrams for each case study.

2.2. Life Cycle Assessment (LCA)

LCA has been widely used to evaluate the environmental performance of biohydrogen production systems by quantifying impacts beyond direct greenhouse gas (GHG) emissions. Key environmental impact categories considered in these studies include global warming potential (GWP), acidification potential (AP), eutrophication potential, ecotoxicity (both terrestrial and freshwater), photochemical ozone formation potential, cumulative non-renewable energy demand (CED), resource depletion, and water consumption, among others [23]. This report aims to provide an expert-level synthesis of these environmental indicators as measured by LCA, drawing on comprehensive studies that consider both conventional and innovative biomass gasification routes.

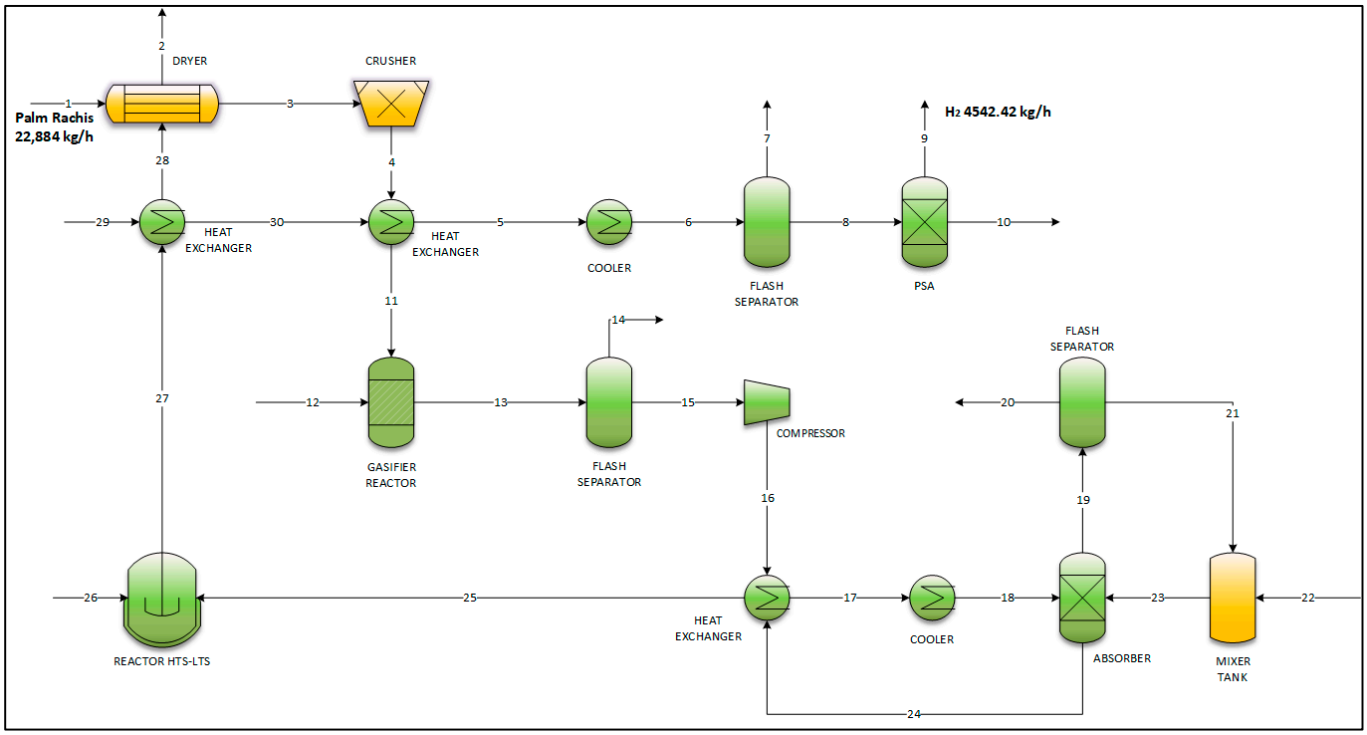

Figure 1. Process Equipment Diagram for the Hydrogen Production Process—Bolivar Case Study.

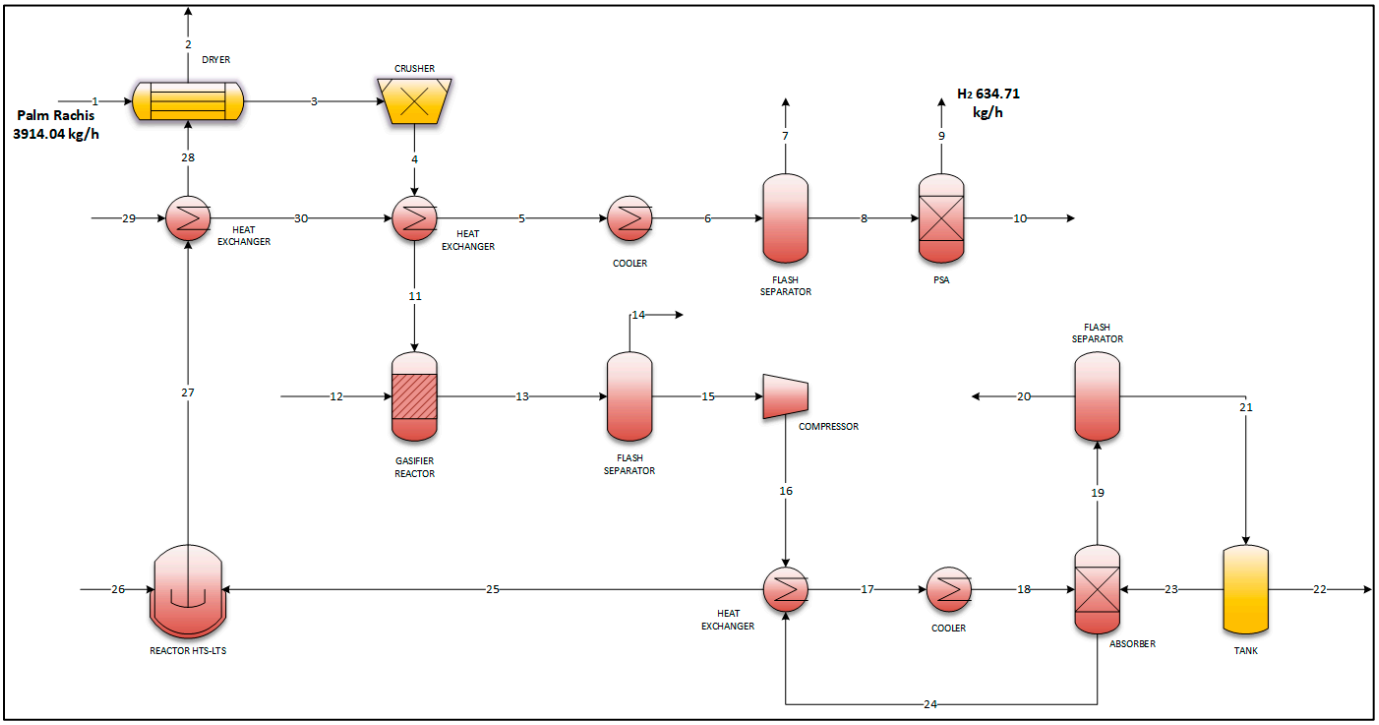

Figure 2. Process Equipment Diagram for the Hydrogen Production Process—Santander Case Study.

The application of LCA to biohydrogen production typically follows the ISO 14040 and ISO 14044 framework [24,25], encompassing goal and scope definition, life cycle inventory (LCI) analysis, life cycle impact assessment (LCIA), and results interpretation. LCAs for biomass gasification systems are generally conducted under cradle-to-gate or cradle-to-grave boundaries, with system boundaries spanning feedstock acquisition, pretreatment, gasification, syngas cleaning, hydrogen separation (often via pressure swing

adsorption), and ancillary processes such as CO_2 removal, heat recovery, and by-product management [26]. Various LCIA methods, including Impact 2002+, ReCiPe 2016, and CML, have been applied to quantify environmental impacts across a range of categories, using functional units often normalized to 1 MWh or 1 kg of hydrogen produced [26,27]. The impact categories were selected using the ReCiPe 2016 Midpoint (H) method, with a focus on indicators relevant to agro-industrial processes and thermal energy systems to ensure a comprehensive assessment of both global decarbonization potential and local environmental footprints. In many cases, LCA studies incorporate system expansion techniques to account for multifunctionality (e.g., simultaneous energy or material recovery from refuse-derived fuels or avoided burdens from waste incineration) and to benchmark biohydrogen against alternative low-carbon hydrogen production routes, such as blue hydrogen from natural gas reforming with CCS or green hydrogen from water electrolysis [23].

Goal and Scope Definition: A rigorous LCA study always begins with a clear definition of the goal and scope. In the case of converting palm oil rachis into hydrogen, the goal is to evaluate the environmental burdens associated with the entire production process, from biomass collection to hydrogen output, with an emphasis on decision-making during the early design phase. It is essential to define the functional unit carefully; for instance, one may choose "1 kg of hydrogen produced" as the functional unit to standardize the results [27]. The system boundaries defined in the present research comprise gate-to-gate operations, biomass pretreatment, gasification, syngas cleaning, and hydrogen separation. Ancillary processes, such as heat recovery and by-product management, are also included within the assessment boundaries.

Regarding the carbon balance, CO_2 uptake via photosynthesis during the oil palm cultivation stage was accounted for within the biogenic carbon cycle framework. Although the specific agricultural phase lies outside the 'gate-to-gate' system boundary (consistent with the selected cut-off approach), the rachis's carbon content is recognized as having been originally sequestered from the atmosphere. Consequently, all CO_2 emissions resulting from the gasification and reforming processes were classified specifically as Biogenic CO_2. In accordance with IPCC guidelines and the ReCiPe methodology, these emissions are distinguished from fossil-derived CO_2, as they belong to a short carbon cycle and do not contribute to the net accumulation of atmospheric greenhouse gases over the long term. Figure 3 represents the system boundaries for the environmental assessment. In orange color we present the inputs in the system and in blue the exits.

Life Cycle Inventory (LCI): A key innovation in this methodology is the use of Aspen Plus simulation to provide high-fidelity mass and energy balances of the palm oil rachis-to-hydrogen conversion process. Aspen Plus is a process simulation tool that generates detailed data on material streams, energy requirements, operating conditions (e.g., temperatures, pressures), and emissions from each process unit. This data, referred to as the foreground system data, serves as the quantitative foundation for the LCI [28]. The simulation outputs cover all critical process parameters, including feedstock consumption rates, conversion efficiencies, waste generation, and energy consumption. To complement the detailed foreground inventory, secondary data on upstream processes (e.g., utility generation) were sourced from a well-documented life-cycle database. Ecoinvent 3 provides standardized, peer-reviewed data, ensuring consistency across studies and facilitating benchmarking against similar processes [29,30]. The Life Cycle Inventory (LCI) was compiled using the 'Allocation, cut-off by classification' system model from the Ecoinvent database. This approach was selected as it is the standard framework for waste valorization studies; it assigns the environmental burdens of upstream agricultural activities (cultivation and extraction) entirely to the primary product (crude palm oil), allowing the rachis to enter the hydrogen production system as a 'burden-free' waste stream that only incurs impacts

from its collection, transport, and conditioning. Although the 'Allocation at the Point of Substitution' (APOS) model is a feasible alternative, it was not adopted in this analysis because it would require allocating a share of agricultural impacts to the residue based on economic or physical relationships. Such an allocation would unnecessarily penalize the biohydrogen pathway with upstream burdens unrelated to the waste management process, thereby obscuring the specific environmental performance of the conversion technology. It is also crucial that any allocation methods, such as economic allocation or system expansion via substitution approaches, are transparently documented and aligned with the chosen LCA methodology [29].

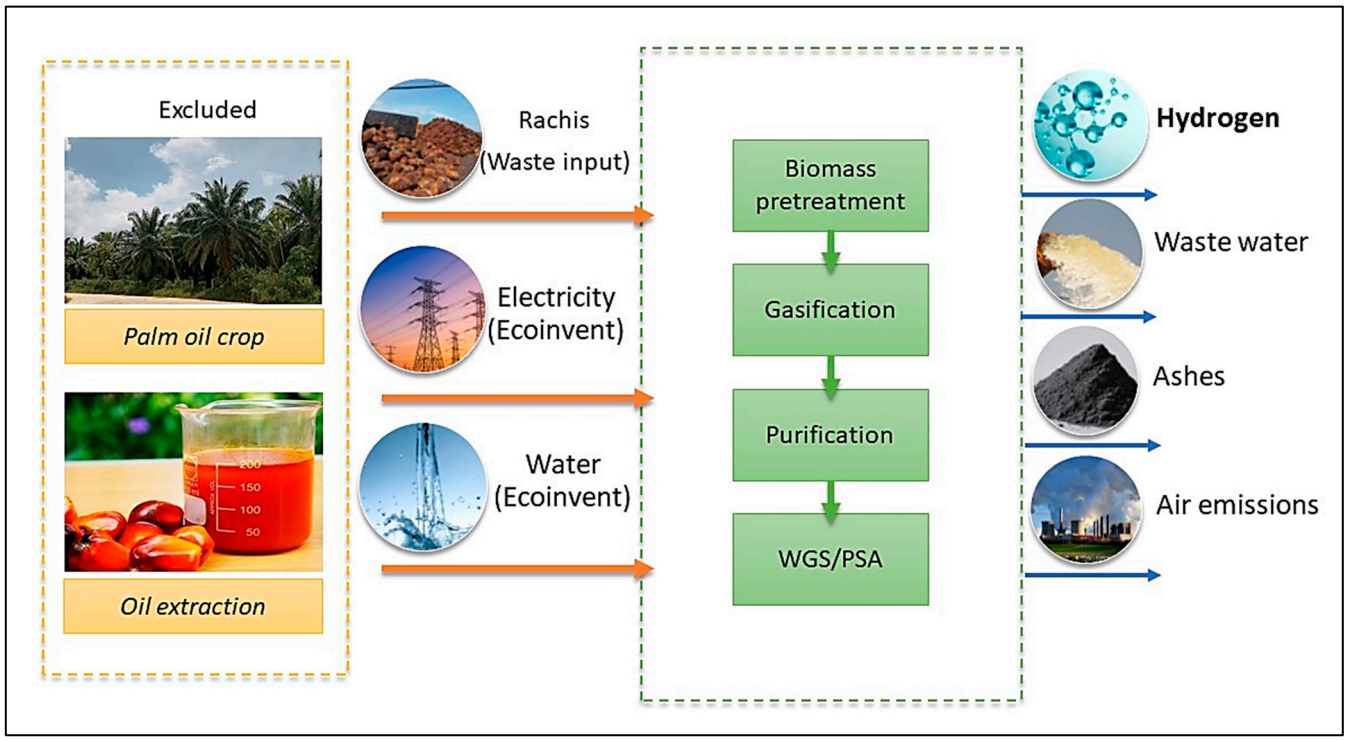

Figure 3. Gate-to-Gate System Boundaries for the Environmental Assessment.

Life Cycle Impact Assessment (LCIA): With the complete LCI in place, the next step is to quantify environmental impacts using an LCIA. A comprehensive LCIA should consider a wide range of environmental aspects, including global warming potential, acidification, eutrophication, resource depletion, photochemical ozone creation, and toxicity potential. Standardized impact assessment methodologies, such as ReCiPe, are recommended, as they have been widely applied in bioenergy LCA studies [27]. The attributional LCA (aLCA) is more straightforward and better suited to this study because it compares technologies under similar conditions [31]. The LCIA is typically implemented using SIMAPRO 10.2 LCA software tools that integrate the previously developed LCI with the chosen impact assessment methods. The present study uses SIMAPRO 10.2. Given the inherent uncertainties associated with emerging technologies, it is essential to conduct sensitivity analyses of key process parameters and assumptions regarding data quality and system boundaries [32,33]. In the present study, two scenarios were considered: in the first, no allocation was applied to processes based on the main product rule; in the second, mass allocation was applied. To evaluate the robustness of the environmental assessment, a sensitivity analysis was conducted focusing on the methodological choice of co-product allocation, in accordance with ISO 14044 recommendations. This analysis compared the baseline scenario (no allocation) with a mass-allocation approach, quantifying how the partitioning of environmental burdens between hydrogen and valuable co-products (biochar and CO_2) affects the final

impact profile. Regarding uncertainty, although a stochastic assessment was outside the scope of this work, data uncertainty was minimized by prioritizing high-fidelity foreground inventories derived directly from rigorous steady-state process simulations (Aspen Plus®). This approach ensures that the Life Cycle Inventory (LCI) is based on thermodynamically consistent mass and energy balances specific to the physicochemical properties of the rachis from Bolívar and Santander, rather than relying on generic average data.

2.3. Economic Evaluation

Economic analysis identifies the financial conditions that jeopardize a production process; for instance, increases in the price of the product, raw materials, or utilities, fluctuations in interest rates, or a decline in product demand, among other factors [34]. This type of assessment facilitates the identification of the investment required for equipment acquisition, site preparation, and start-up costs, among others. This constitutes the Total Capital Investment (TCI), as expressed in Equation (1), where FCI represents the funds required for equipment payments, land preparation, control systems, etc.; WCI corresponds to Working Capital Investment; and SUC denotes Start-Up Costs. Similarly, Operating Costs (OC) can be determined using Equation (2); these correspond to the continuous expenses required for the operation of a production plant [35]. The cost of operating labor was estimated following the heuristic method described by Turton et al. [36]. The number of operators required per shift was calculated based on the number of major processing steps, including particulate and non-particulate operations. To reflect the study's specific context, the base salary was defined using current Colombian labor market data for skilled industrial technicians, set at approximately 30 USD/h (fully burdened). This rate accounts for continuous 24/7 operation, requiring 4.5 shift teams to cover weekends, holidays, and leave.

$$TCI = FCI + WCI + SUC \tag{1}$$

$$OC = DPC + FCH + POH + GE \tag{2}$$

$$VPN = \sum_{n} AFC_n (1 + i)^{-n} \tag{3}$$

$$PBP = \frac{FCI}{PAT} \tag{4}$$

$$\%ROI = \frac{PAT}{TCI} \times 100\% \tag{5}$$

Furthermore, economic evaluation yields indicators such as the Net Present Value (NPV), the Payback Period (PBP), and the Return on Investment (ROI), as shown in Equations (3)–(5), respectively. These indicators are employed to analyze process changes and the time value of money [37].

3. Results and Discussion

3.1. Results of Process Simulation

Table 3 summarizes the electricity, cooling water, and products for both study cases. As previously presented, the Santander biomass has an unusually high elemental hydrogen content (9.42%) compared to Bolivar (6.58%). Theoretically, a higher H/C ratio in the feedstock should facilitate higher hydrogen yields and lower reforming energy requirements. Still, the results show that, although the Bolivar plant processes 5.8 times more biomass, it produces 7.1 times more Hydrogen. This non-linearity indicates that the efficiency gap is not merely a simulation artifact but a thermodynamic consequence of the feedstock properties and process scale. Specifically, the Santander biomass contains nearly four times as much ash (5.69%) as the Bolívar sample. Mechanistically, this inert fraction acts as a thermal sink

inside the reactor, absorbing sensible heat and lowering the effective reaction temperature. Since steam methane reforming is strongly endothermic ($\Delta H°298$ K = +206 kJ/mol), even small decreases in temperature shift the chemical equilibrium toward the reactants, thereby preventing the complete liberation of the feedstock's hydrogen. To improve performance in the Santander scenario, two operational adjustments are recommended: (1) implementing a rigorous Heat Exchanger Network (HEN) to recover the 3.47 kW/kg of thermal energy currently dissipated in the cooling train, recycling it to preheat the feed; and (2) adopting an auto-thermal gasification strategy. By introducing a controlled oxidant stream (air or oxygen), the process could generate in situ heat via partial oxidation, thereby compensating for the thermal inertia of the ash and sustaining the high temperatures required for optimal reforming kinetics.

Table 3. Simulation results summary.

Parameter	Bolivar Process	Santander Process
Hydrogen obtained (kg/h)	4542.41	634.71
Electricity consumption (kW)	27,830.92	14,982.6
Cooling service (kW)	8891.83	13,612.61
Ash (kg/h)	271.58	137.87
CO_2-rich stream (kg/h)	52,132.33	6785.9

By normalizing energy consumption against the input mass flow, we can assess the efficiency of the equipment handling the solid biomass. The cooling duty of 3.47 kW/kg of biomass is extraordinarily high. This suggests that the Santander gasifier or reformer is operating at excessively high temperatures without heat recovery, or that the syngas cooling train is oversized and inefficient. In contrast, Bolivar's 0.39 kW/kg indicates a tightly integrated Heat Exchanger Network (HEN) in which hot syngas preheats the feed or steam.

The Aspen Plus® simulation indicates that the higher ash content of Santander biomass (5.69 wt% vs. 1.39 wt% in Bolívar) requires greater sensible heat to raise the solids to the gasification temperature. This results in an 8–12% increase in the reactor's thermal load. However, this alone cannot explain why the electricity consumption per kilogram of biomass processed is about 3.2 times higher in Santander (3.82 kWh/kg versus 1.22 kWh/kg in Bolívar).

First, the high cooling duty calculated in the simulation (13,612 kW) points to a lack of effective heat integration. In a well-optimized gasification–steam methane reforming (SMR) system, typically 45–55% of the sensible heat in the hot syngas (800–900 °C) is recovered internally, for example, to preheat the biomass, generate process steam, or raise the reformer inlet temperature. In contrast, the Santander model discharges almost all this heat to coolers, resulting in a specific cooling demand of 3.47 kW per kilogram of biomass. This is nearly nine times the value seen in the Bolívar simulation (0.39 kW/kg). This suggests that the Santander process relies heavily on electrical heaters rather than on internally recovered heat to achieve the necessary operating temperatures for the gasifier and reformer. Since electric heating is generally 2–4 times less efficient than heat recovery or combustion-based heating, this aligns with the elevated power demand predicted by Aspen. Second, the syngas composition predicted by the Aspen model after gasification shows lower-than-expected yields of CO and H_2. This implies suboptimal operating conditions, such as an improper steam-to-biomass ratio or inadequate temperature control in the gasifier. The resulting incomplete carbon conversion forces the system to handle larger

volumes of syngas, thereby increasing both compression and cooling duties and raising overall energy use.

Figure 4 shows the simulation workflow for the two processes analyzed. Because raw materials differ by the extraction technologies implemented at the plants, the quantity of rachis available for hydrogen production varies across plants. The rachis production rate at the Bolivar plant is 22,884 kg/h, whereas at Santander it is 3919.04 kg/h.

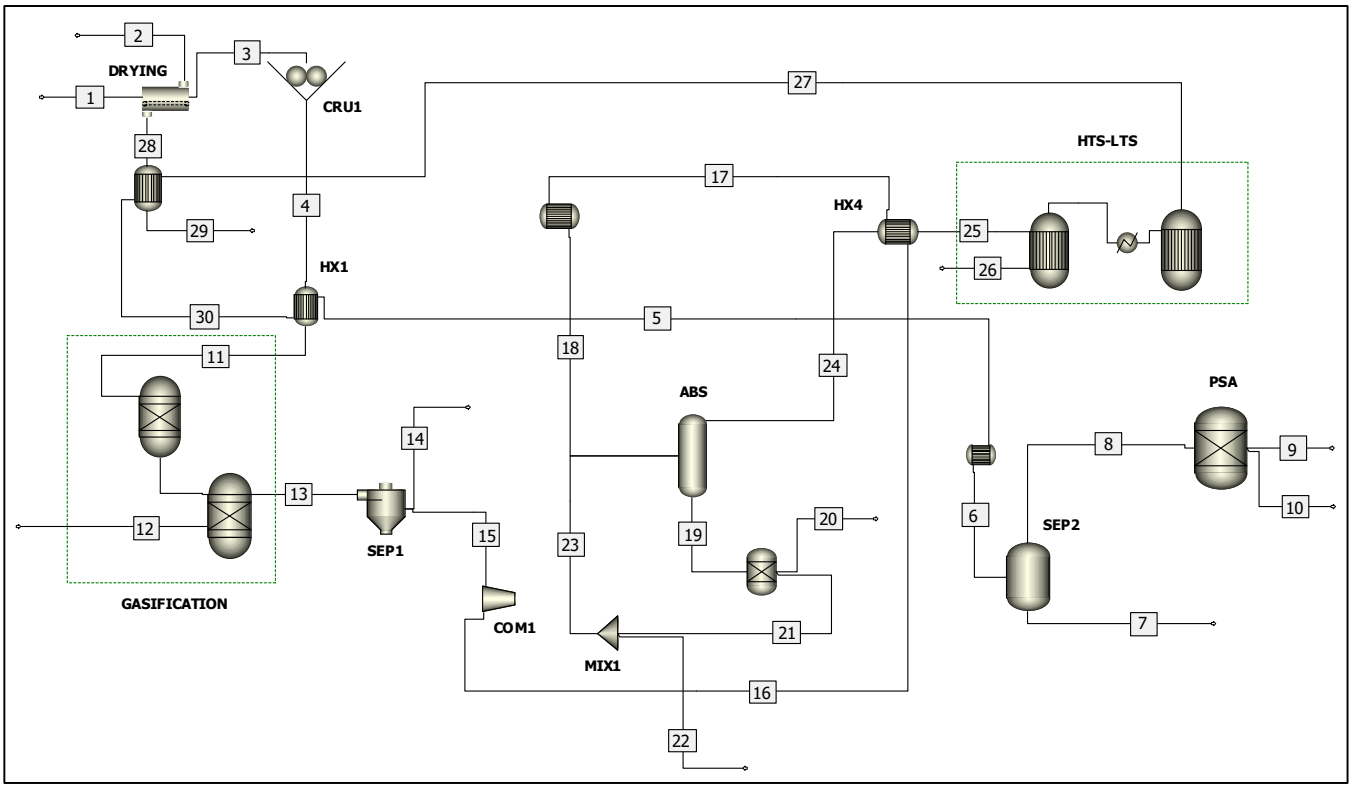

Figure 4. Simulation workflow and process pathway for hydrogen production from both feedstocks.

Methane production: Since it was not possible to establish a reliable reaction equation to describe the decomposition of biomass in the first gasifier, whose primary objective is to generate methane (CH_4) as a precursor for subsequent synthesis, a non-stoichiometric RYield reactor was selected. The decomposition yields were taken from Macdonald et al. [38], enabling the disaggregation of biomass into its fundamental constituents. At this initial stage, the primary products formed were solid carbon (C), hydrogen gas (H_2), ash (ASH), and elemental sulfur (S). No significant formation of methane (CH_4), carbon monoxide (CO), carbon dioxide (CO_2), or water (H_2O) was observed, consistent with the characteristic behavior of an elemental decomposition reactor and confirming that methane must be produced in a subsequent gasification step.

The solid and gaseous products from the decomposition stage were subsequently routed to a second gasifier. This unit was modeled following the approach proposed by Stefano Lange et al. [3] and operated with superheated steam at a flow rate of 4600 kg/h and a temperature of 900 °C. Under these high-temperature steam gasification conditions, the reactor generated product streams enriched in key combustible species, particularly carbon monoxide (CO), methane (CH_4), and carbon dioxide (CO_2), along with water vapor (H_2O), sulfur dioxide (SO_2), and ash (ASH). In contrast, the flows of hydrogen (H_2), oxygen (O_2), and nitrogen (N_2) remained negligible.

These results demonstrate that the second-stage gasifier effectively converts solid carbon into synthesis gases, including methane, thus fulfilling its intended role within

the hydrogen production pathway [39]. The reactor operated at approximately 900 °C, 60 bars, and a steam-to-biomass molar ratio of 1.2:1, parameters widely recognized for promoting methane formation and improving syngas quality [40,41]. Under these operating conditions, the simulation predicted a methane yield of approximately 0.33 mol CH_4 per mole of Rachis fed, resulting in a high-calorific syngas composition [42,43]. This conversion performance corresponds to a Cold Gas Efficiency (CGE) of 60% for the Santander scenario and 78% for the Bolívar scenario. While the Santander result aligns perfectly with the validated range of 50–60% reported in the literature for similar steam-blown fluidized-bed gasifiers processing lignocellulosic biomass [42,44], the Bolívar scenario exhibits superior energy recovery. This higher efficiency is attributable to the significantly lower ash content of the Bolívar feedstock (1.39% vs. 5.69%), which minimizes thermal inertia in the reactor. Consequently, these quantitative indicators confirm that the proposed design maximizes energy transfer to the gas phase while minimizing carbon losses to char.

Washing and product separation process: After leaving the gasifier, the gaseous stream is directed to a separation unit modeled using the RadFrac block in Aspen Plus. At this stage, a freshwater stream at 30 °C is introduced at a molar ratio of 0.5:1 relative to the incoming gas flow. The purpose of this operation is to promote the absorption of condensable species and acid gases present in the syngas, while allowing non-condensable gases, such as methane, carbon monoxide, and carbon dioxide, to proceed to subsequent stages of the process. The column was configured with 10 theoretical stages, providing adequate mass transfer and ensuring stable composition profiles throughout the equipment. Under these operating conditions, the absorption step removes approximately 30% of the CO_2 and 26% of the SO_2 from the incoming stream. A controlled purge stream is withdrawn from the bottom of the absorber to remove accumulated contaminants and the solvent.

The RadFrac block represents the most rigorous Aspen Plus model for equilibrium-based column operations, as it simultaneously solves the material balance, energy balance, phase equilibrium, and Equations of State, collectively known as the MESH equations [45]. This approach enables an accurate representation of vapor–liquid mass-transfer phenomena and allows prediction of the distribution of each component across all stages of the column. In this configuration, the column operates in absorption mode, meaning neither a condenser nor a reboiler is specified, since the objective is physical removal of contaminants rather than fractional distillation. To accurately represent the system's thermodynamic behavior, an activity coefficient-based model, such as NRTL, was selected for its ability to describe highly nonideal systems comprising water, sulfur dioxide, carbon dioxide, and residual organic compounds [46]. The use of such a model is essential for capturing the critical intermolecular interactions present in aqueous mixtures containing acid gases [47]. During the simulation, Aspen Plus computes phase equilibrium at each theoretical stage, enabling precise predictions of temperature, composition, and internal flow profiles. As a result, the overhead stream of the RadFrac column is enriched in methane and carbon monoxide, making it suitable for subsequent conversion or purification steps within the hydrogen production pathway. In contrast, the bottom stream concentrates the absorbed species primarily water, sulfur dioxide, soluble carbon, and other compounds with a higher affinity for the liquid phase.

Methane reforming to hydrogen: The final stage of the process is carried out using two equilibrium reactors modeled in Aspen Plus through the REquil block. This reactor type employs a rigorous equilibrium-based formulation in which the outlet stream composition is determined by minimizing the system's Gibbs free energy at the specified temperature and pressure [48]. Rather than requiring predefined stoichiometric equations, the REquil model identifies all feasible reactions among the defined chemical species and calculates the equilibrium composition that satisfies the laws of mass action and thermody-

namic consistency [48]. This makes the model particularly suitable for high-temperature reforming systems in which multiple reactions co-occur, such as steam methane reforming, Water–Gas Shift, and methane cracking [49]. In Aspen Plus, the REquil reactor solves the equilibrium state by performing a global energy and mass balance and applying equilibrium constants derived from the selected thermodynamic property method. For methane reforming, the model accounts for key reactions including $CH_4 + H_2O \rightleftharpoons CO + 3H_2$ and $CO + H_2O \rightleftharpoons CO_2 + H_2$, ensuring that the thermodynamic limits at the chosen operating conditions govern all conversions [50]. In this process configuration, a gas-to-steam molar ratio of 1:5 was used, with the reforming reactors operating at approximately 1000 °C, conditions that strongly favor endothermic methane reforming. Under these high-temperature, steam-rich conditions, the system achieves a methane conversion of 91.3%, a value observed consistently across both scenarios evaluated. This high conversion efficiency is characteristic of equilibrium-limited reforming processes. It indicates that the operational parameters—temperature, steam ratio, and reactor configuration—are appropriate for maximizing hydrogen production while minimizing residual methane.

Supplementary Equipment: A fundamental part of the process, thermal conditioning is performed using heat exchangers modeled with the HeatX block in Aspen Plus. This model rigorously solves the energy balances between two streams without mass transfer, computing thermal profiles and heat duties using global heat-transfer coefficients and thermodynamic properties calculated at each operating point [51]. For equipment sizing and energy integration, the overall heat-transfer coefficients (U) were estimated based on the fluid phases and stream properties. A coefficient of 500 W/(m^2 K) was applied to water-cooled coolers and steam heaters, whereas 50 W/(m^2 K) was used for gas-gas heat exchangers. For the compression stages, the units were modeled with an isentropic efficiency of 0.75 and a mechanical efficiency of 0.95, typical of centrifugal compressors in industrial gas-processing applications [40]. This configuration allows the system to recover thermal gradients generated during critical stages, such as gasifier outlet cooling, the high-temperature shift reactor (HTS), and subsequent purification steps [52]. The recovered heat is transferred to the water and steam streams feeding the methane reforming reactors, significantly reducing external energy demand and improving the overall energetic efficiency of the process. Heat exchangers such as HX1 and HX4, and the coolers associated with streams 18 and 23, play a central role in this thermal circuit, conditioning the process streams to prevent overheating of sensitive equipment and to ensure suitable conditions for absorption and downstream separation operations.

In addition to the heat exchangers, the process incorporates compressors, with COM1 being the most relevant. These units were modeled as polytropic compressors, using the polytropic work equation coupled with energy balance equations that account for predefined mechanical and adiabatic efficiencies. The compressors increase the gas pressure before it enters units that are highly sensitive to operating pressure, such as the HTS reactor, the absorption columns, and the PSA unit. Maintaining the process stream within the optimal pressure range is critical to favor the kinetics of the Water–Gas Shift (WGS) reaction and ensure effective separation in the Pressure Swing Adsorption (PSA) unit. To achieve this, the compression stages were modeled in Aspen Plus using a rigorous isentropic compression method. The simulation assumed an isentropic efficiency of 75% and a mechanical efficiency of 95%, values that adhere to standard heuristics for industrial centrifugal compressors. Subsequently, the PSA unit was modeled to enable hydrogen purification, considering a multilayer adsorbent bed composed of activated carbon and zeolites, designed to selectively adsorb impurities from the synthesis gas while allowing hydrogen to pass through. The PSA design criteria focused on achieving a hydrogen purity

of 99.9%, with an overall hydrogen recovery between 80 and 90%, in accordance with industrial practice and the performance reported in the literature [53].

The process also includes several separation vessels, such as SEP1, SEP2, and the auxiliary separators associated with streams 6, 7, 14, and 15. These units are modeled in Aspen Plus using Flash2 separators, in which vapor–liquid equilibrium is solved using the selected thermodynamic model, enabling accurate prediction of phase distribution and stream compositions. SEP1 plays a critical role by removing condensed water, fine carbonaceous particles, and heavy compounds formed after the gasifier cooling step. SEP2, in turn, handles the liquid stream enriched in CO_2, SO_2, and other soluble compounds generated during the absorption stage. The presence of multiple separation drums stabilizes intermediate flows and prevents droplet or mist carryover that could compromise compressor operation and PSA performance. To ensure correct integration of the process flows, mixers such as MX1 and mixing nodes represented by streams 5, 17, and 19 are included. These units are simulated using isobaric mixing blocks that solve algebraic mass and energy balances, without chemical kinetics or phase-equilibrium calculations. Their function is to homogenize recycled, conditioned, or purged flows before they enter reactors and separation units, ensuring that each section receives streams with stable temperatures, compositions, and flow rates.

Additionally, stable operation of the water and steam circuits is maintained through internal recirculations implemented using Design Specs and Adjust Blocks in Aspen Plus V14. These tools automatically adjust operating variables, such as water flow rate, recycle fraction, or heat duty, to meet specific process criteria (e.g., setting the reformer inlet temperature or controlling the steam-to-gas ratio). This configuration ensures that the system operates within the desired thermodynamic boundaries, compensating for fluctuations in composition or flow rate of the principal streams.

3.2. LCA

The objective of the LCA was to evaluate environmental indicators for the two processes and compare the results of both methods with data reported in the literature and in the Ecoinvent database. The functional unit selected was 1 kg of hydrogen, and the system boundaries set were "gate to gate". The allocation method used was mass allocation; the impact assessment methodology was Recipe; and the categories measured were global warming potential, fine particulate matter formation, terrestrial acidification, freshwater eutrophication, freshwater ecotoxicity, water consumption, and fossil resource scarcity. Although the study excludes upstream biomass production and downstream hydrogen use, the gasification stage involves energy inputs, air emissions, effluents, and auxiliary resource consumption that are effectively captured through these categories under the ReCiPe Midpoint 2016 (H) methodology.

Tables 4 and 5, contain the mass and energy balances results obtained from the Aspen Plus simulations. These data were then entered into SimaPro 10.2 to model inventory analysis and conduct impact category evaluation.

Table 4. Mass flows in the inventory analysis.

Process/Stream *	1	2	3	4	5	6
H_2 Bolivar (kg/h)	22,884.38	27,837.61	5932.99	5932.99	57,136.32	57,136.32
H_2 Santander (kg/h)	3919.04	1927.18	3011.85	3011.85	14,029.05	14,029.05
Process/Stream *	7	8	9	10	11	12
H_2 Bolivar (kg/h)	462.17	56,674.15	4541.74	52,132.41	5932.99	1515
H_2 Santander (kg/h)	6608.45	7420.60	634.71	6785.90	3011.85	5443.11

Table 4. *Cont.*

Process/Stream *	13	14	15	16	17	18
H_2 Bolivar (kg/h)	7447	2948.86	4499.12	4499.12	4499.12	4499.12
H_2 Santander (kg/h)	8454.96	137.87	8317.10	8317.10	8317.10	8317.10
Process/Stream *	19	20	21	22	23	24
H_2 Bolivar (kg/h)	21,676.66	6526.92	15,149.75	9.07	10,894.64	46,250.11
H_2 Santander (kg/h)	6081.45	1840.65	4240.80	2721.55	2721.55	4957.20
Process/Stream *	25	26	27	28	29	30
H_2 Bolivar (kg/h)	46,250.11	10,886.22	57,136.32	10,886.22	10,886.22	57,136.32
H_2 Santander (kg/h)	4957.20	9071.85	14,029.05	1020.00	1020.00	14,029.05

* The number of the streams comes from Figures 1 and 2.

Table 5. Energy flows in the inventory analysis.

Electricity Consumption (kW)		
Equipment	**Hydrogen Bolivar**	**Hydrogen Santander**
CRUS	20.00	20.00
C3	7852.36	5897.84
GASIF	300.00	300.00
HTS-LTS	25,054.60	9953.6
COM1	2456.32	4709.00
C1	1039.47	7714.77
Total	36,722.75	28,595.21

During the inventory analysis in SimaPro 10.2, the steam, cooling-water, and electricity flows were modeled using the Ecoinvent 3 database. For the steam flow, the selected option was Steam in the chemical industry, RoW, cut-off system. For cooling water, the process used was *Tap water*, *CO*, *cut-off system*. Finally, for electricity consumption, the chosen option was *Electricity*, *low voltage*, *CO*, *cut-off system*. The Cut-off system model was selected over the Cut-off unit model because it aligns more closely with the methodological principles of attributional life cycle assessment (A-LCA), which focuses on describing the environmental burdens directly associated with the product system under study. Under the Cut-off system approach, recycled materials and wastes enter the system without burden. At the same time, the environmental impacts of recycling processes are allocated to the product that generates the recyclable material. This treatment avoids double-counting of impacts and provides a transparent representation of material flows. For these reasons, the use of the Cut-off system ensures methodological consistency, transparency in burden allocation, and greater comparability with other studies using Ecoinvent 3. The results for the impact evaluation are shown in Table 6.

Table 6. LCIA results without applying mass allocation to byproducts.

Impact Category	Units	Hydrogen Bolivar	Hydrogen Santander
Global warming potential (GWP)	kg CO_2 eq	2.467	15.031
Fine particulate matter formation	kg PM2.5 eq	0.003	0.018
Terrestrial acidification	kg SO_2 eq	0.009	0.048
Freshwater eutrophication	kg P eq	0.001	0.004

Table 6. *Cont.*

Impact Category	Units	Hydrogen Bolivar	Hydrogen Santander
Freshwater ecotoxicity	kg 1,4-DCB	0.241	1.071
Fossil resource scarcity	kg oil eq	0.604	3.890
Water consumption	m^3	0.372	3.798

Considering the lower heating value of hydrogen (33.3 kWh/kg H_2), the GWP expressed per unit of energy corresponds to 74.15 kg CO_2-eq/MWh for the Bolívar case and 451.38 kg CO_2-eq/MWh for the Santander case. Studies indicate that biohydrogen produced via biomass gasification can exhibit substantially lower GWP values than fossil pathways, often resulting in net negative emissions when biogenic carbon uptake during biomass growth is appropriately accounted for, and Carbon Capture and Storage (CCS) technologies are applied [54]. For scenarios that integrate Carbon Capture and Storage (CCS), the absorption unit was modeled assuming a carbon capture efficiency of 90%. This value represents the standard performance for commercial-scale chemical absorption systems using monoethanolamine (MEA) or activated methyldiethanolamine (MDEA) as the solvent. While higher capture rates are theoretically feasible, standard techno-economic guidelines for hydrogen production with CCS recommend a 90% baseline to balance energy penalties with environmental benefits [55,56]. Furthermore, some innovative configurations—such as integrating waste biomass from municipal solid waste (MSW)—have demonstrated climate-change benefits of approximately −419 kg CO_2-eq./MWh from avoided emissions relative to conventional incineration [23]. Conversely, scenarios without CCS or those that neglect biogenic carbon yield positive GWP figures, highlighting the sensitivity of LCA outcomes to assumptions about feedstock quality and process integration [23]. Table 7 presents a benchmarking analysis of the palm rachis gasification process. The results indicate that the Bolívar scenario achieves hydrogen yield and energy efficiency comparable to the upper tier of reported values for agricultural residues, likely due to the optimized feedstock quality (low ash content). Environmentally, both scenarios demonstrate a substantial reduction in carbon footprint relative to the fossil-based Steam Methane Reforming (SMR) benchmark (~11 kg CO_2/kg H_2), validating the decarbonization potential of the proposed pathway. Economically, although the LCOH is higher than that of fossil hydrogen, it remains competitive with reported bio-hydrogen production costs, particularly for the large-scale scenario.

Table 7. Comparison of Results with Previous Studies.

Indicator	Units	This Study (Bolivar)	This Study (Santander)	Reaño et al. [39]	Lepage et al. [37]	Fossil SMR (Benchmark)
H_2 Yield	g H_2/kg Biomass	198.4972033	161.9571319	71.7	40–130 (Steam Gasification), 40–190 (General gasification)	No data
Cold Gas Eff. (CGE)	%	78.0	60.0	50.3	Not Reported	>75
GWP	kg CO_2-eq/kg H_2	2.47	15.031	2.42	Not Reported	10–12
LCOH	USD$/kg$H_2$	2.6–3.2	3.2–3.8	Not Reported	1.21–3.5	1.5–2.5

Fine Particulate Matter Formation and Terrestrial Acidification are strongly influenced by gaseous emissions (NO_x, SO_2, particulates) associated with thermochemical conversion. For both categories, Bolívar shows an impact lower than Ecoinvent's, whereas Santander

consistently performs worse (see Figure 5). This pattern indicates that, in the Santander case, emissions control or operating conditions result in greater atmospheric impacts. These categories are significant for gasification projects because air emissions represent a key environmental concern for thermochemical systems.

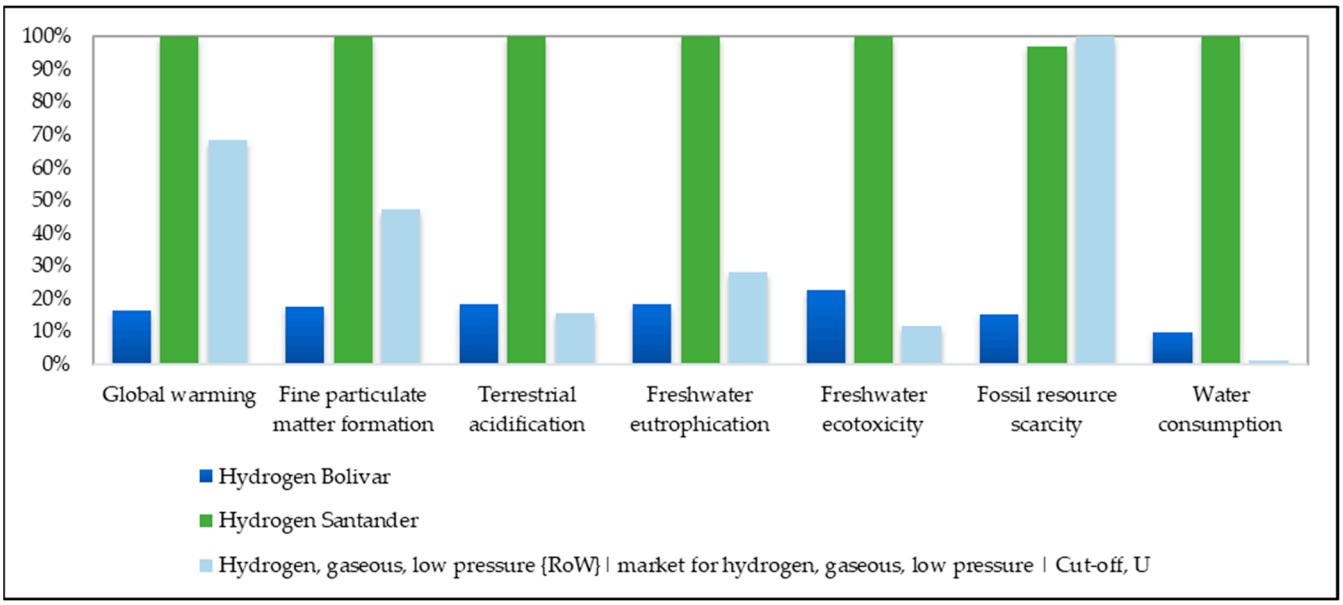

Figure 5. Normalized Life Cycle Impact Assessment (LCIA): Bolivar vs. Santander vs. Ecoinvent.

Eutrophication potential quantifies the risk of nutrient enrichment in aquatic ecosystems, typically expressed in kg P equivalents. In biohydrogen LCAs from biomass gasification, eutrophication impacts are influenced by upstream inputs, such as fertilizer use during biomass cultivation, as well as by combustion-related emissions [54,57]. While some pathways, particularly those using waste feedstocks, may indirectly benefit from avoided impacts associated with conventional waste treatment, the overall eutrophication potential can remain significant, necessitating careful management of nutrient releases [54]. In the freshwater eutrophication indicator, Bolívar again outperforms Ecoinvent, whereas Santander exceeds both Bolívar and the reference value. Given that gasification may involve condensates and water-based cleaning systems, this indicator is relevant for assessing local water-quality risks.

Ecotoxicity impacts are assessed in the freshwater compartment and are often expressed as comparative toxic units (e.g., CTUe or kg 1,4-DCB equivalents). The ecotoxicity potential of biohydrogen production processes is strongly influenced by the release of toxic substances during biomass pretreatment, gasification, and syngas cleaning; for instance, emissions of chemicals used in scrubbers and filters (e.g., sodium hypochlorite) are of particular concern [26]. Furthermore, studies have indicated that although the direct toxicity of the hydrogen product may be minimal, indirect contributions from upstream emissions associated with the processing of MSW or agricultural residues can increase ecotoxicity scores [58,59]. In the present research, freshwater ecotoxicity shows the most pronounced deviations. The Bolívar case more than doubles the Ecoinvent value, and the Santander case exceeds it by nearly an order of magnitude. This suggests that the handling of tars, trace metals, or wastewater streams in both case studies—particularly in Santander—may impose significant ecotoxicological burdens. For biomass gasification, this category is essential because contaminants from syngas cleaning can substantially influence freshwater ecosystems if not properly managed.

In contrast, Fossil Resource Scarcity performs better than Ecoinvent in both case studies, with Bolívar showing the lowest impact. Since the feedstock is a residual biomass and energy inputs may be lower or partially renewable, this result indicates a reduced dependency on fossil resources, reinforcing the attractiveness of biomass-based hydrogen pathways. Water management is an increasingly pertinent issue in LCAs, particularly for processes with high steam and cooling demands such as biomass gasification. Biohydrogen LCAs have quantified the water consumption potential (WCP) and water scarcity footprints (WSF), which account for regional water resource availability [54]. While gasification generally requires less freshwater than biological processes such as dark fermentation, substantial water inputs for drying, steam generation, and cooling can still be significant, particularly if water recycling is not optimally implemented [44]. Santander's water demand is substantially higher than the Ecoinvent benchmark, while Bolívar performs moderately above the reference value. Because gasification requires water for steam generation, cooling, and cleaning stages, this indicator is crucial for assessing the feasibility of deployment in regions with water constraints. The results suggest that water management strategies in Santander may require optimization.

While numerous LCA studies consistently demonstrate that biohydrogen produced via biomass gasification can achieve significant benefits, including reduced GWP and lower fossil resource consumption, compared with conventional hydrogen production methods, these benefits often come with trade-offs. The acidification potential and ecotoxicity impacts tend to be higher in some configurations, particularly when the gasification process involves extensive syngas cleaning and the use of chemicals in filters and scrubbers [26]. The energy inputs required to attain high operating temperatures (typically 700–1200 °C) and to drive separation and purification processes can increase the cumulative non-renewable energy demand if not managed through integrated heat-recovery systems [56]. Moreover, environmental performance is sensitive to key process parameters, including feedstock moisture content, biomass composition (e.g., the biogenic carbon fraction, which can vary between 40 and 60%), and the efficiency of CO_2 capture and utilization methods. Sensitivity analyses in these studies underscore that improvements in process efficiency, optimization of operating conditions, and substitution of fossil-based energy inputs with renewable sources can effectively mitigate several of the observed environmental burdens [23].

Several LCAs have benchmarked biohydrogen produced via biomass gasification against other low-carbon hydrogen production pathways, such as blue hydrogen via steam methane reforming with CCS and green hydrogen from water electrolysis powered by renewable energy sources. In many comparative studies, biohydrogen offers a distinct advantage for climate change mitigation, owing to its net-negative or highly reduced GWP when biogenic carbon is accounted for [23]. However, while biohydrogen tends to perform well on GWP metrics, its acidification potential and specific ecotoxicity parameters sometimes remain comparable to, or even slightly exceed, those of its fossil-based counterparts. For example, studies indicate that acidification potentials in biohydrogen routes can be up to 4–22% higher than those for blue or green hydrogen, largely due to the indirect environmental burdens introduced by syngas cleaning processes [60]. Other impact categories, such as cumulative non-renewable energy demand and resource depletion, also display favorable performance in biohydrogen systems when energy recovery measures are integrated and when the renewable character of the feedstock is effectively harnessed [60]. Overall, the comparative LCAs reinforce the view that, while biohydrogen from biomass gasification is a desirable option for climate change mitigation, concerted efforts to optimize processes are essential to mitigate residual impacts across other environmental domains [54].

A recurring theme in LCA studies of biohydrogen production via biomass gasification is the considerable uncertainty surrounding metering and system boundaries. Variations in

biomass moisture content, feedstock composition (particularly the biogenic carbon fraction), energy supply mix, and the efficiency of process units such as gasifiers and syngas cleaning systems can lead to a wide range of reported environmental impact values [23]. Sensitivity analyses are thus critical tools that enable researchers to explore the effects of these variables and identify environmental hotspots in which process improvements will yield the greatest benefits [44]. Furthermore, integrating multifunctional LCA approaches—where co-products such as recovered metals, biochar, and excess electricity are credited—can improve the apparent eco-efficiency of the system but requires careful justification and transparent methodological choices [53,60].

The previous LCIA results were calculated without mass allocation to co-products, as the primary product and motivation of the processes is hydrogen production. Table 8 presents the results for a more favorable process scenario, with two co-products: char coal and a CO_2-rich stream. The allocation method used is based on mass. In this new scenario, both processes have better environmental indicators than the hydrogen reference selected from the Ecoinvent database. Within the water consumption category, hydrogen from Santander still has the highest impact indicator (see Figure 6).

Table 8. LCIA results applying mass allocation to byproducts.

Impact Category	Units	Hydrogen Bolivar	Hydrogen Santander
Global warming potential (GWP)	kg CO_2 eq	0.196	1.280
Fine particulate matter formation	kg PM2.5 eq	2.45×10^{-4}	0.001
Terrestrial acidification	kg SO_2 eq	0.001	0.004
Freshwater eutrophication	kg P eq	5.50×10^{-5}	0.0003
Freshwater ecotoxicity	kg 1,4-DCB	0.019	0.091
Fossil resource scarcity	kg oil eq	0.048	0.331
Water consumption	m^3	0.030	0.323

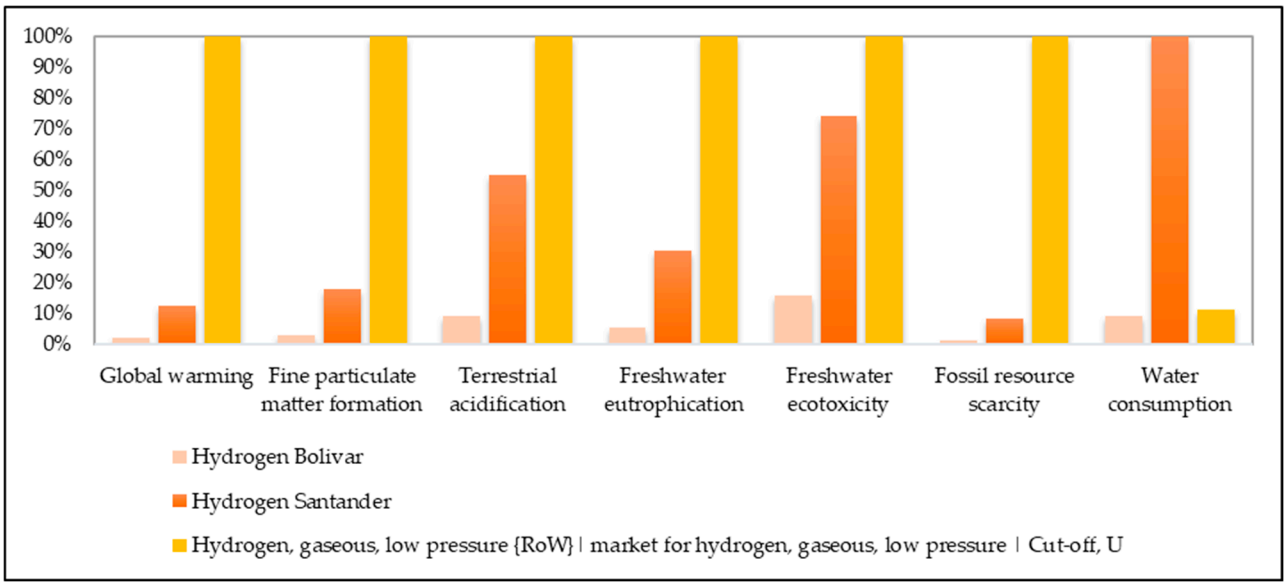

Figure 6. Normalized Life Cycle Impact Assessment (LCIA) with mass allocation: Bolivar vs. Santander vs. Ecoinvent.

3.3. Techno-Economic Evaluation

A cost of 50 USD/t was considered for palm rachis, and a price of 3100 USD/t for hydrogen [61]. Since the process does not use reagents to produce hydrogen, no other raw materials were considered. Regarding industrial utilities, the process primarily consumes water, steam, electricity, and compressed air. Table 9 outlines the key considerations for installing a hydrogen production plant using palm rachis in the Department of Bolívar, specifically in María La Baja, and a second plant in the Department of Santander, located in Sabana de Torres. This biomass is typically used for energy generation. Furthermore, a plant service life of 15 years was established, with a tax rate of 35% [62] and an interest rate of 10% [63] for the year 2025. Additionally, a contingency value of 36% was set, representing funds reserved for strikes, design changes, price fluctuations, and floods.

Table 9. Techno-economic considerations for the hydrogen production plants based on palm rachis.

Considerations	Value/Description
Processing capacity (t/y)	22.88 Bolivar case study; 3.91 Santander case study
Main product flow rate (t/y)	4.54 Bolivar case study; 0.634 Santander case study
Raw material cost ($/t)	50
Main product price ($/t)	3100
Plant service life (years)	15
Salvage value	10% of depreciable FCI
Plant construction time	2 years
Tax Rate (ITR)	35%
Discount rate	10%
Process type	New process
Process control	Digital
Soil type	Soft clay
Contingency percentage (%)	36
Tank design code	(ASME)
Utilities	Water, steam, electricity, air
Operator hourly cost (US$/h)	30

A computer-aided techno-economic assessment was conducted using the techno-economic analysis methodology developed by Romero et al. [35]. The Total Capital Investment was calculated, along with Economic Potentials (EP), Cumulative Cash Flow (CCF), Payback Period (PBP), Return on Investment (ROI), Net Present Value (NPV), and the annual Benefit–Cost Ratio. Table 10 presents a detailed report on the total investment items for the hydrogen production plant in 2025, including equipment installation costs, piping, electrical systems, and other components. Equipment prices for the processes were obtained from supplier quotations (www.alibaba.com) during the research.

Table 11 presents the total operating costs associated with implementing the palm rachis-based hydrogen production plant in 2025. These costs encompass labor, maintenance, raw materials, taxes, and industrial utilities, among others. The operating costs account for Direct Production Costs (DPC), Fixed Charges (FCH), Plant Overhead (POH), and General Expenses (GE). Specifically, this includes operation-related expenses contingent on production capacity; expenses independent of operations or production capacity, such as

taxes, security services, general engineering, internal transport, and medical services; and administrative, marketing, and research and development expenses, among others.

Table 10. Total Capital Investment for the hydrogen production plant based on palm rachis.

Item	Bolivar (US$ 2025)	Santander (US$ 2025)	Applied Factor (%)
Purchased Equipment Cost	1,987,400.00	1,892,200.00	2 × FOB price
Purchased Equipment Installation	775,086.00	737,958.00	39
Instrumentation and Controls (installed)	258,362.00	245,986.00	13
Piping (installed)	616,094.00	586,582.00	31
Electrical Systems (installed)	198,740.00	189,220.00	10
Service Facilities	1,093,070.00	1,040,710.00	55
Total DFCI	**4,928,752.00**	**4,692,656.00**	**-**
Yard Improvements	258,362.00	245,986.00	13
Engineering and Supervision	635,968.00	605,504.00	32
Equipment (R + D)	198.740	189,220.00	10
Construction Expenses	675,716.00	643,348.00	34
Legal Expenses	19,874.00	18,922.00	1
Contractor's Fee	345,012.64	328,485.92	7
Contingency	715,464.00	681,192.00	36
Total IFCI	**2,849,136.64**	**2,712,657.92**	**-**
Fixed Capital Investment (FCI)	7,777,888.64	7,405,313.92	-
Working Capital Investment (WCI)	1,555,577.73	1,481,062.78	20
Start-Up Costs (SUC)	777,788.86	740,531.39	10
Total Capital Investment (TCI)	**10,111,255.23**	**9,626,908.1**	**-**

Bold: total calculation of DFCI, IFCI and TCI.

Table 11. Annual operating costs of the hydrogen production process from palm rachis.

Item	Bolivar (US$ 2025)	Santander (US$ 2025)
Raw materials	9,153,600.00	1,728,000.00
Industrial Services (Utilities)	88,334,782.44	9,268,914.00
Total VAOC	**97,488,382.44**	**10,996,913.61**
Local taxes	233,336.66	222,159.42
Insurance	77,778.89	74,053.14
Interest/Rent	101,112.55	96,269.08
Total FCH	**412,228.10**	**392,481.64**
Maintenance and repairs	388,894.43	370,265.70
Operating supplies	58,334.16	55,539.85
Operating labor	1,935,733.33	1,935,733.33
Direct supervision and clerical labor	290,360.00	290,360.00
Laboratory charges	193,573.33	193,573.33
Patents and royalties	77,778.89	74,053.14

Table 11. *Cont.*

Total DPC	**2,944,674.15**	**2,919,525.36**
Overhead (POH)	1,161,440.00	1,161,440.00
General expenses (GE)	1,026,528.54	1,020,241.34
Annualized Operating Costs (AOC)	**103,033,253.22**	**16,490,601.94**

Bold: total calculation of FCH, DPC and AOC.

The profitability analysis was driven by the revenue obtained from the sale of biohydrogen. Consequently, after deducting the Annual Operating Costs (AOC) and applying a 35% corporate tax rate, the resulting net cash flow enables recovery of the initial capital investment in 4.54 years. This relatively short payback period is attributed to the low cost of the feedstock (residue) and the high energy efficiency of the gasification process, which minimizes utility expenses.

Table 12 displays the economic and profitability indicators. A Net Present Value (NPV) of USD 25.01 million and a Benefit–Cost Ratio of 3.29 were obtained. The Benefit–Cost Ratio serves as a key indicator of project feasibility; in this instance, the project is deemed viable because the indicator exceeds 1.

Table 12. Economic and profitability indicators for the hydrogen production process from palm rachis.

Indicator (Year 2025)	**Value (Bolivar)**	**Value (Santander)**
Cumulative Cash Flow or CCF (1/year)	0.95	−0.08
Discounted Payback Period or DPBP (years)	4.54	−32.68
%ROI	58.83%	−8.06%
NPV (millions of USD)	25.01	−10.25
Internal Rate of Return or IRR	38.13%	-
Benefit–Cost Ratio	3.29	−1.35
Profitability Indicators	**Value (US$)**	**Value (US$)**
Gross Profit or GP	9,618,514.78	−749,793.94
Gross Profit with Depreciation or DGP	9,151,841.46	−1,194,112.78
Profit After Taxes or PAT	5,948,696.95	−776,173.31
EBITDA	10,085,188.10	−305,475.11

It is relevant to consider the implications of an alternative scenario in which the process is terminated at the methane production stage (Synthetic Natural Gas, SNG), bypassing the conversion to hydrogen. From a capital investment perspective, excluding the Steam Methane Reforming (SMR), Water–Gas Shift (WGS), and PSA units would reduce the Fixed Capital Investment (FCI) by approximately 30–40%, as gas conditioning and separation are capital-intensive operations. However, this reduction in CAPEX does not necessarily translate into higher profitability. The market price of natural gas (methane) is substantially lower than that of high-purity hydrogen on an energy-equivalent basis. Moreover, producing SNG would align the project with fossil fuel substitutes rather than the high-value decarbonization market. Therefore, while the 'methane-only' route offers a lower barrier to entry in terms of investment, the proposed 'hydrogen pathway' maximizes both the specific revenue per ton of biomass and the environmental value added.

To evaluate how the process responds to potential changes in key economic parameters, a techno-economic resilience analysis was performed. This approach enables assessment of hydrogen production from palm rachis under scenarios with increased feedstock prices

and varying plant performance conditions. It also provides insight into the operational thresholds at which the process becomes economically infeasible. Figures 7 and 8 present the sensitivity analysis of economic stability by plotting the On-Stream Efficiency at the Break-Even Point (BEP) against the hydrogen selling price for both case studies. In both cases, the curves exhibit an explicit inverse, non-linear relationship: as the selling price of hydrogen increases, the minimum on-stream efficiency required to cover total costs decreases. In other words, higher product prices confer greater economic flexibility, whereas lower prices require stricter operational performance.

Figure 7. On-stream efficiency at the break-even point at Bolivar's plant.

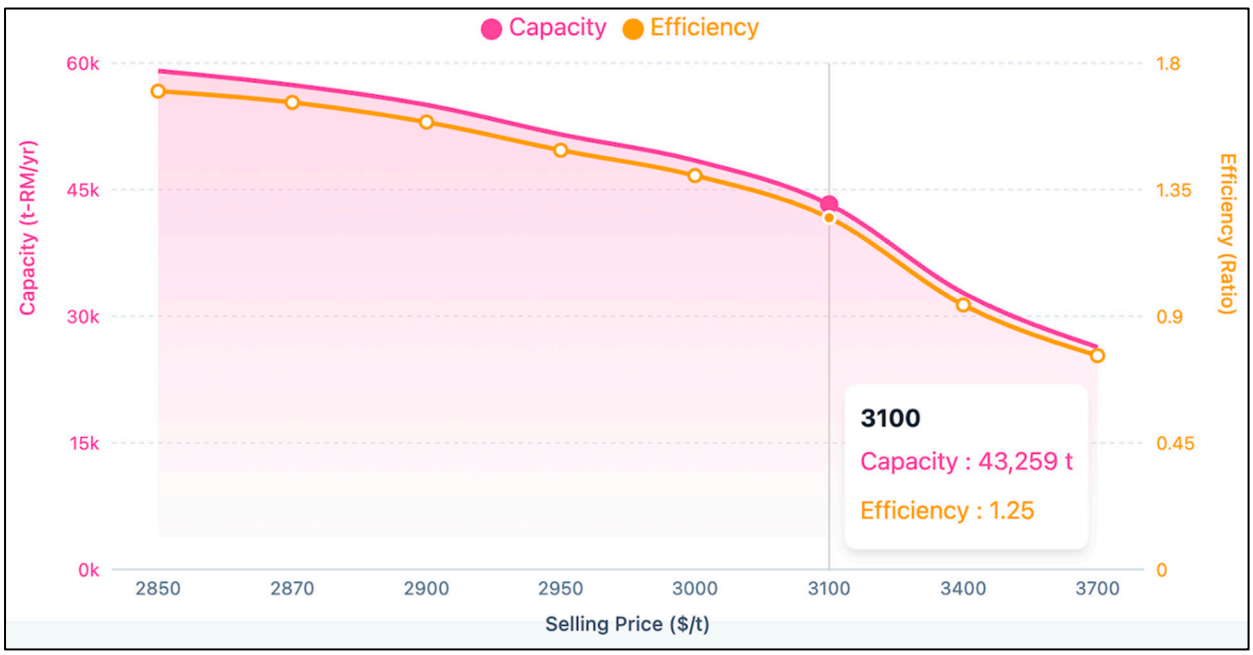

Figure 8. On-stream efficiency at the break-even point at Santander's plant.

For the Bolívar plant (Figure 7), the base-case selling price of USD 3100 per t corresponds to a required on-stream efficiency of 39.65% to reach the BEP. This relatively low value indicates a robust operational margin, suggesting the plant can remain economically viable even with moderate reductions in availability, downtime, or performance.

In contrast, the Santander plant (Figure 8) exhibits a markedly less favorable resilience profile. At the same selling price of USD 3100/t, the required on-stream efficiency rises to 125.17%, a physically unattainable level. This result highlights the economic vulnerability of the Santander configuration: even under optimistic selling-price conditions, the process cannot achieve cost recovery without substantial improvements in technology performance, operational conditions, or economic assumptions. Overall, the comparison underscores that hydrogen production from palm rachis is economically promising in regions with conditions like Bolívar—where biomass availability, logistics, and operational parameters are favorable—while regions resembling the Santander scenario face substantial barriers that must be addressed before such projects can be considered feasible.

4. Conclusions

This study presented an integrated technical, environmental, and economic assessment of hydrogen production from palm oil rachis in two Colombian post-conflict regions (Bolívar and Santander). By combining detailed Aspen Plus simulations, a gate-to-gate environmental Life Cycle Assessment, and a comprehensive techno-economic evaluation, the work provides a holistic understanding of the feasibility and sustainability of this biohydrogen pathway.

The results reveal a marked contrast between the two case studies in terms of process performance. While the Aspen Plus simulation validated the thermochemical route of gasification integrated with steam methane reforming (SMR) as an effective technology, a critical non-linearity was identified between feedstock quality and process yield. The Bolívar configuration demonstrates superior performance, achieving a mass conversion efficiency of 0.198 kg H_2/kg biomass and better heat integration via an optimized Heat Exchanger Network. In contrast, the Santander configuration exhibits substantial inefficiencies. Despite a feedstock with a higher elemental hydrogen content (9.42% on a dry basis) than Bolívar (6.58%), it suffers from poor conversion performance and poor heat management, limiting its capacity to utilize the available hydrogen in the biomass.

Environmentally, the Bolívar process consistently outperforms both the Santander configuration and the Ecoinvent hydrogen benchmark in most impact categories, particularly regarding global warming potential and fossil resource scarcity. This consolidates the Bolívar route as a sustainable pathway toward green/blue hydrogen production. Conversely, the Santander process exhibits significant environmental burdens, particularly in water consumption and ecotoxicity, driven by a high specific demand for industrial services and by greater ash generation per unit of product. However, when co-product mass allocation is applied, both configurations show improved environmental performance, with the Bolívar system achieving values below the Ecoinvent reference in nearly all categories.

The economic assessment confirms that production scale is the governing variable for the financial viability of biomass gasification. The Bolívar plant exhibits strong financial viability, characterized by a discounted payback period of 4.54 years, a positive Net Present Value (NPV) of USD 25.01 million, a Return on Investment (ROI) of 58.83%, and a Benefit–Cost Ratio of 3.29. The sensitivity analysis further highlights the resilience of the large-scale process, which requires a moderate on-stream efficiency (~40%) to break even. Conversely, the Santander plant is not economically feasible under current conditions, showing negative profitability indicators and extreme vulnerability; it would

require an unattainable on-stream efficiency of over 125% at the base-case hydrogen price to become profitable.

Overall, the results indicate that hydrogen production from palm rachis is a sustainable and competitive alternative in regions with favorable biomass availability, logistics, and operational conditions, such as Bolívar. In such post-conflict zones, this technology acts as a catalyst for regional economic development, mitigating agro-industrial liabilities and generating a high-tech value chain aligned with the Sustainable Development Goals, specifically regarding affordable clean energy and climate action. However, locations resembling the Santander case face significant challenges that must be addressed through process redesign or the adoption of decentralized biorefinery models rather than complete in situ gasification plants. Consequently, future work will focus on experimental validation of the simulated pathways and on optimizing supply chain logistics to enhance the economic viability of small-scale implementations. This work underscores the strategic potential of residual biomass valorization while highlighting the need for context-specific design strategies to ensure environmental and financial sustainability.

Author Contributions: Conceptualization, P.A.A.P. and Á.D.G.-D.; methodology, P.A.A.P. and T.C.H.-R.; software, P.A.A.P. and T.C.H.-R.; validation, P.A.A.P. and T.C.H.-R.; formal analysis, P.A.A.P. and T.C.H.-R.; investigation, P.A.A.P. and T.C.H.-R.; resources, Á.D.G.-D.; data curation, P.A.A.P. and T.C.H.-R.; writing—original draft preparation, P.A.A.P. and T.C.H.-R.; writing—review and editing, P.A.A.P., T.C.H.-R. and Á.D.G.-D.; visualization, Á.D.G.-D.; supervision, Á.D.G.-D.; project administration, Á.D.G.-D.; funding acquisition, Á.D.G.-D. All authors have read and agreed to the published version of the manuscript.

Funding: This research was funded by the Colombian Ministry of Science, Technology and Innovation MINCIENCIAS through the projects "Desarrollo e implementación de una metodología para evaluar aspectos sociales, técnicos, económicos y ambientales de la producción de hidrógeno a partir de raquis de palma en Sabana de Torres y María la Baja", Code SIGP 100459, Contract 352-2023.

Institutional Review Board Statement: Not applicable.

Informed Consent Statement: Not applicable.

Data Availability Statement: The data that support the findings of this study are available from the corresponding author, Á.D.G.-D., upon reasonable request.

Acknowledgments: The authors thank the Universidad de Cartagena for technical support. Paola Andrea Acevedo Pabón thank to Federico López and EAN university for the technical support in parts of the simulation. Ángel Darío González-Delgado thanks Luis Angel González-Fontalvo for providing curiosity, motivation and inspiration for continuing research during these 9 months.

Conflicts of Interest: The authors declare no conflicts of interest.

References

1. Tuntiwongwat, T.; Srinophakun, T.R.; Sukpancharoen, S. Computational Thermodynamic Analysis of Hydrogen Production via Biomass Gasification. In *2024 International Conference on Advanced Robotics and Mechatronics (ICARM), Tokyo, Japan, 6–8 July 2024*; IEEE: Piscataway, NJ, USA, 2024; pp. 715–720. [CrossRef]
2. Harahap, R.K.; Nur, T.B.; Syafiie, S. Aspen Plus Simulation Analysis of Hydrogen Production from Biomass Pyrolysis Integrated with Steam Methane Reformer Unit. In *IOP Conference Series: Earth and Environmental Science*; IOP Publishing: Bristol, UK, 2024; pp. 1–7. [CrossRef]
3. Langè, S.; Pellegrini, L.A. Economic Analysis of a Combined Production of Hydrogen-Energy from Empty Fruit Bunches. *Biomass Bioenergy* **2013**, *59*, 520–531. [CrossRef]
4. Arenas, C.N.; Bello, A.P.; Molina, N.F.; Botero, J.L.; Betancur, M. A Social Life Cycle Assessment as a Key to Territorial Development: A Study of the Hydrangea Crop in Colombia. *Sustainability* **2024**, *16*, 4156. [CrossRef]
5. Hosseini, S.E.; Wahid, M.A.; Ganjehkaviri, A. An Overview of Renewable Hydrogen Production from Thermochemical Process of Oil Palm Solid Waste in Malaysia. *Energy Convers. Manag.* **2015**, *94*, 415–429. [CrossRef]

6. Cardona-Alzate, C.A.; Serna-Loaiza, S.; Ortiz-Sanchez, M. Sustainable Biorefineries: What Was Learned from the Design, Analysis and Implementation. *J. Sustain. Dev. Energy Water Environ. Syst.* **2020**, *8*, 88–117. [CrossRef]
7. Solarte, J.C. Oil Palm Rachis Gasification for Synthesis Gas Production. 2017. Available online: https://repositorio.unal.edu.co/handle/unal/63870 (accessed on 28 July 2025).
8. Dzulkarnain, E.L.N.; Audu, J.O.; Wan Dagang, W.R.Z.; Abdul-Wahab, M.F. Microbiomes of Biohydrogen Production from Dark Fermentation of Industrial Wastes: Current Trends, Advanced Tools and Future Outlook. *Bioresour. Bioproc.* **2022**, *9*, 16. [CrossRef] [PubMed]
9. Dreyer, L.C.; Hauschild, M.Z.; Schierbeck, J. A Framework for Social Life Cycle Impact Assessment. *Int. J. Life Cycle Assess.* **2006**, *11*, 88–97. [CrossRef]
10. Hussain, M.; Tufa, L.D.; Yusup, S.; Zabiri, H. A Kinetic-Based Simulation Model of Palm Kernel Shell Steam Gasification in a Circulating Fluidized Bed Using Aspen Plus®: A Case Study. *Biofuels* **2018**, *9*, 635–646. [CrossRef]
11. Costa, T.; Monteiro, A.; Vicente, J.; Vasconcelos, A.; Malveira, M. Survey of Technical-Economic Perspectives and Challenges for the Green Hydrogen Market in Brazil. In *2023 15th IEEE International Conference on Industry Applications (INDUSCON)*; IEEE: Piscataway, NJ, USA, 2023; pp. 372–377. [CrossRef]
12. Al-Malah, K.I.M. *Aspen Plus®: Chemical Engineering Applications*; John Wiley & Sons, Inc.: Hoboken, NJ, USA, 2017; p. 623, ISBN 978-1-119-13123-6. [CrossRef]
13. Abdelouahed, L.; Authier, O.; Mauviel, G.; Corriou, J.P.; Verdier, G.; Dufour, A. Detailed Modeling of Biomass Gasification in Dual Fluidized Bed Reactors under Aspen Plus. *Energy Fuels* **2012**, *26*, 3840–3855. [CrossRef]
14. Sandler, S.I. A Rigorous Distillation Calculation: RadFrac. In *Using Aspen Plus in Thermodynamics Instruction: A Step-by-Step Guide*; Wiley: Hoboken, NJ, USA, 2015; pp. 252–271. Available online: https://www.wiley.com/en-us/Using+Aspen+Plus+in+Thermodynamics+Instruction%3A+A+Step-by-Step+Guide-p-9781118996911 (accessed on 20 November 2025).
15. Tavares, R.; Monteiro, E.; Tabet, F.; Rouboa, A. Numerical Investigation of Optimum Operating Conditions for Syngas and Hydrogen Production from Biomass Gasification Using Aspen Plus. *Renew. Energy* **2020**, *146*, 1309–1314. [CrossRef]
16. Çepelioğullar Mutlu, Ö.; Zeng, T. Challenges and Opportunities of Modeling Biomass Gasification in Aspen Plus: A Review. *Chem. Eng. Technol.* **2020**, *43*, e202000068. [CrossRef]
17. Marcantonio, V.; Monforti Ferrario, A.; Di Carlo, A.; Del Zotto, L.; Monarca, D.; Bocci, E. Biomass Steam Gasification: A Comparison of Syngas Composition between a 1-D MATLAB Kinetic Model and a 0-D Aspen Plus Quasi-Equilibrium Model. *Computation* **2020**, *8*, 86. [CrossRef]
18. Sierra, V.; Ceballos, C.; Chejne Janna, F. Simulation of Thermochemical Processes in Aspen Plus as a Tool for Biorefinery Analysis. *CT&F-Cienc. Tecnol. y Futuro* **2021**, *11*, 2. [CrossRef]
19. Petrescu, L.; Cormos, C.C. Waste Reduction Algorithm Applied for Environmental Impact Assessment of Coal Gasification with Carbon Capture and Storage. *J. Clean. Prod.* **2015**, *104*, 220–235. [CrossRef]
20. *UNE-EN 15407:2011*; Combustibles Sólidos Recuperados. Métodos para la Determinación del Contenido de Carbono (C), Hidrógeno (H) y Nitrógeno (N). Asociación Española de Normalización (UNE): Madrid, Spain, 2011.
21. *ASTM D5622-95*; Standard Test Methods for Determination of Total Oxygen in Gasoline and Methanol Fuels by Reductive Pyrolysis. ASTM International: West Conshohocken, PA, USA, 1995.
22. Krotz, L.; Giazzi, G. *Thermo Scientific™ Application Note 42151: Elemental Analysis: CHNS/O Characterization of Biomass and Bio-Fuels*; Thermo Fisher Scientific: Waltham, MA, USA, 2017.
23. Amaya-Santos, G.; Chari, S.; Sebastiani, A.; Grimaldi, F.; Lettieri, P.; Materazzi, M. Biohydrogen: A Life Cycle Assessment and Comparison with Alternative Low-Carbon Production Routes in UK. *J. Clean. Prod.* **2021**, *319*, 128886. [CrossRef]
24. *ISO 14040:2006*; Environmental Management—Life Cycle Assessment—Principles and Framework. International Organization for Standardization (ISO): Geneva, Switzerland, 2006.
25. *ISO 14044:2006*; Environmental Management—Life Cycle Assessment—Requirements and Guidelines. International Organization for Standardization (ISO): Geneva, Switzerland, 2006.
26. Gonzalez-Delgado, A.D.; Parejo, V.; Herrera, T. Computer-Aided Environmental Evaluation of Bio-Hydrogen Production from Residual Biomass of Palm Cultivation. *Contemp. Eng. Sci.* **2017**, *10*, 773–783. [CrossRef]
27. Moreno, J.; Iglesias, J.; Blanco, J.; Montero, M.; Morales, G.; Melero, J.A. Life-Cycle Sustainability of Biomass-Derived Sorbitol: Proposing Technological Alternatives for Improving the Environmental Profile of a Bio-Refinery Platform Molecule. *J. Clean. Prod.* **2020**, *250*, 119568. [CrossRef]
28. Mio, A.; Barbera, E.; Massi Pavan, A.; Bertucco, A.; Fermeglia, M. Sustainability Analysis of Hydrogen Production Processes. *Int. J. Hydrogen Energy* **2024**, *54*, 540–553. [CrossRef]
29. Antonini, C.; Treyer, K.; Moioli, E.; Bauer, C.; Schildhauer, T.J.; Mazzotti, M. Hydrogen from Wood Gasification with CCS—A Techno-Environmental Analysis of Production and Use as Transport Fuel. *Sustain. Energy Fuels* **2021**, *5*, 2602–2621. [CrossRef]

30. Antonini, C.; Treyer, K.; Streb, A.; van der Spek, M.; Bauer, C.; Mazzotti, M. Hydrogen Production from Natural Gas and Biomethane with Carbon Capture and Storage—A Techno-Environmental Analysis. *Sustain. Energy Fuels* **2020**, *4*, 2967–2986. [CrossRef]
31. González Mallén, V. Consequential Life Cycle Assessment (cLCA) of Biomass-to-Hydrogen Technologies: The WoodRoll© Case. Available online: www.kth.se (accessed on 27 November 2025).
32. Han, D.; Yang, X.; Li, R.; Wu, Y. Environmental Impact Comparison of Typical and Resource-Efficient Biomass Fast Pyrolysis Systems Based on LCA and Aspen Plus Simulation. *J. Clean. Prod.* **2019**, *231*, 254–267. [CrossRef]
33. Khila, Z.; Baccar, I.; Jemel, I.; Hajjaji, N. Thermo-Environmental Life Cycle Assessment of Hydrogen Production by Auto-Thermal Reforming of Bioethanol. *Energy Sustain. Dev.* **2017**, *37*, 66–78. [CrossRef]
34. Herrera, T.; Parejo, V.; Gonzalez, A. Technoeconomic Sensibility Analysis of Industrial Agar Production from Red Algae. *Chem. Eng. Trans.* **2018**, *70*, 2029–2034. [CrossRef]
35. Romero, J.; Vergara, L.; Peralta, Y.; González, A. A Techno-Economic Sensitivity Approach for Development of Palm-Based Biorefineries in Colombia. *Chem. Eng. Trans.* **2017**, *57*, 13–18. [CrossRef]
36. Turton, R.; Bailie, R.C.; Whiting, W.B.; Shaeiwitz, J.A. *Analysis, Synthesis, and Design of Chemical Processes*, 3rd ed.; Prentice Hall PTR: Upper Saddle River, NJ, USA, 2009; ISBN 978-0-13-512966-1.
37. El-Halwagi, M. *Sustainable Design Through Process Integration: Fundamentals and Applications to Industrial Pollution Prevention, Resource Conservation, and Profitability Enhancement*; Elsevier: Amsterdam, The Netherlands, 2011.
38. Macdonald, J.H.; Mohd Paad, K.; Kamaruzaman, N.; Yamanaka, S.; Abbas, A.; Abdul Manaf, N. Robust Simulation Platform of Biomass Gasification Process with Carbon Capture for Energy Vector Polygeneration. *Chem. Eng. Trans.* **2024**, *113*, 535–540. [CrossRef]
39. López Muñoz, F.; Meramo, S.; Ricardez-Sandoval, L.; Gonzalez, A.D.; Crissien Castillo, B.; Gonzalez Quiroga, A.; Baptiste, B.L.G.; León-Pulido, J. Insights from an exergy analysis of a green chemistry chitosan biorefinery. *Chem. Eng. Res. Des.* **2023**, *194*, 666–677. [CrossRef]
40. Towler, G.; Sinnott, R. *Chemical Engineering Design: Principles, Practice and Economics of Plant and Process Design*, 3rd ed.; Elsevier: Oxford, UK, 2021; ISBN 978-0-12-821179-3.
41. Peters, M.S.; Timmerhaus, K.D.; West, R.E. *Plant Design and Economics for Chemical Engineers*, 5th ed.; McGraw-Hill: New York, NY, USA, 2002; ISBN 978-0-07-239266-1.
42. Lepage, T.; Kammoun, M.; Schmetz, Q.; Richel, A. Biomass-to-Hydrogen: A Review of Main Routes Production, Processes Evaluation and Techno-Economical Assessment. *Biomass Bioenergy* **2021**, *144*, 105920. [CrossRef]
43. IRENA. *Green Hydrogen Cost Reduction: Scaling Up Electrolysers to Meet the 1.5 °C Climate Goal*; International Renewable Energy Agency: Abu Dhabi, United Arab Emirates, 2020; ISBN 978-92-9260-295-6.
44. Reaño, R.L. Assessment of Environmental Impact and Energy Performance of Rice Husk Utilization in Various Biohydrogen Production Pathways. *Bioresour. Technol.* **2020**, *299*, 122590. [CrossRef]
45. Dou, J.; Wang, S.; Yao, Z. Mixed Protonic–Electronic Conducting Ceramic Membranes for Hydrogen Separation: A Review on Recent Advances in Structure Optimization and Preparation. *Sep. Purif. Technol.* **2025**, *355*, 129582. [CrossRef]
46. Yi, N.; Herraiz, L.; Fang, M.; García, S.; van der Spek, M. Open Access, Thermodynamically Consistent, Electrolyte NRTL Model for Piperazine, AMP, Water, CO_2 Systems on Aspen Plus. *Sep. Purif. Technol.* **2024**, *350*, 127924. [CrossRef]
47. Esmaeili, A.; Liu, Z.; Xiang, Y.; Yun, J.; Shao, L. Modeling and Validation of Carbon Dioxide Absorption in Aqueous Solution of Piperazine + Methyldiethanolamine by PC-SAFT and E-NRTL Models in a Packed Bed Pilot Plant: Study of Kinetics and Thermodynamics. *Process Saf. Environ. Prot.* **2020**, *141*, 95–109. [CrossRef]
48. Haider, M.B.; Jha, D.; Marriyappan Sivagnanam, B.; Kumar, R. Modelling and Simulation of CO_2 Removal from Shale Gas Using Deep Eutectic Solvents. *J. Environ. Chem. Eng.* **2019**, *7*, 102747. [CrossRef]
49. Li, S.; Li, H.; Yu, Y.; Chen, J. Simulation and Performance Comparison for CO_2 Capture by Aqueous Solvents of N-(2-Hydroxyethyl) Piperazine and Another Five Single Amines. *Processes* **2021**, *9*, 2184. [CrossRef]
50. Song, C.; Clarkson, C.R.; Deglint, M.; Ghanizadeh, A.; Blinderman, M.S.; Evans, C.; Liu, S. Study of Simultaneous Hydrogen Gas Stream Purification and CO_2 Storage in Coal Samples Using an Experimentally Simulated Huff 'n' Puff Scheme Combined with the Rate-Transient Analysis, Porosity, and Permeability Core Analysis Method. *SPE J.* **2025**, *30*, 3861–3880. [CrossRef]
51. Qu, M.; Yan, X.; Wang, H.; Hei, Y.; Liu, H.; Li, Z. Energy, Exergy, Economic and Environmental Analysis of Photovoltaic/Thermal Integrated Water Source Heat Pump Water Heater. *Renew. Energy* **2022**, *194*, 1084–1097. [CrossRef]
52. Singh Yadav, V.; Vinoth, R.; Yadav, D. Bio-Hydrogen Production from Waste Materials: A Review. *MATEC Web Conf.* **2018**, *192*, 02020. [CrossRef]
53. Krótki, A.; Bigda, J.; Spietz, T.; Ignasiak, K.; Matusiak, P.; Kowol, D. Performance Evaluation of Pressure Swing Adsorption for Hydrogen Separation from Syngas and Water–Gas Shift Syngas. *Energies* **2025**, *18*, 1887. [CrossRef]
54. Mehmeti, A.; Angelis-Dimakis, A.; Arampatzis, G.; McPhail, S.J.; Ulgiati, S. Life Cycle Assessment and Water Footprint of Hydrogen Production Methods: From Conventional to Emerging Technologies. *Environments* **2018**, *5*, 24. [CrossRef]

55. Roussanaly, S.; Rubin, E.S.; van der Spek, M.; Booras, G.; Berghout, N.; Fout, T.; Garcia, M.; Gardarsdottir, S.; Kuncheekannah, V.N.; Matuszewski, M.; et al. *Towards Improved Guidelines for Cost Evaluation of Carbon Capture and Storage*; SINTEF Energy Research: Trondheim, Norway, 2021. [CrossRef]
56. Wang, Y.; Zhao, L.; Otto, A.; Robinius, M.; Stolten, D. A Review of Post-Combustion CO_2 Capture Technologies from Coal-Fired Power Plants. *Energy Procedia* **2017**, *114*, 650–665. [CrossRef]
57. Tsalidis, G.A.; El Discha, F.; Korevaar, G.; Haije, W.; de Jong, W.; Kiel, J. An LCA-Based Evaluation of Biomass to Transportation Fuel Production and Utilization Pathways in a Large Port's Context. *Int. J. Energy Environ. Eng.* **2017**, *8*, 175–187. [CrossRef]
58. Li, Q.; Song, G.; Xiao, J.; Hao, J.; Li, H.; Yuan, Y. Exergetic Life Cycle Assessment of Hydrogen Production from Biomass Staged-Gasification. *Energy* **2020**, *190*, 116416. [CrossRef]
59. Loy, A.C.M.; Alhazmi, H.; Lock, S.S.; Yiin, C.L.; Cheah, K.W.; Chin, B.L.; How, B.S.; Yusup, S. Life-Cycle Assessment of Hydrogen Production via Catalytic Gasification of Wheat Straw in the Presence of Straw-Derived Biochar Catalyst. *Bioresour. Technol.* **2021**, *341*, 125796. [CrossRef] [PubMed]
60. Maniscalco, M.P.; Longo, S.; Cellura, M.; Miccichè, G.; Ferraro, M. Critical Review of Life Cycle Assessment of Hydrogen Production Pathways. *Environments* **2024**, *11*, 108. [CrossRef]
61. Alibaba. Pure Hydrogen—Gases CAS 1601346006195. 2025. Available online: https://www.alibaba.com/product-detail/China-Makes-Special-Specialty-Gases-CAS_1601346006195.html (accessed on 20 November 2025).
62. Actualícese. General Income Tax Rate 2025 for Legal Entities. 2024. Available online: https://actualicese.com/tarifa-general-del-impuesto-de-renta-2025-para-personas-juridicas/ (accessed on 20 November 2025).
63. World Bank. Interest Rate (%). 2025. Available online: https://data.worldbank.org/indicator/FR.INR.RINR (accessed on 6 November 2025).